An Evaluation of Air Pollutant Exposures due to the 1991 Kuwait Oil Fires using a Lagrangian Model

Roland R. Draxler, Jeffery T. McQueen, Barbara J.B. Stunder
National Oceanic and Atmospheric Administration
Air Resources Laboratory
1315 East West Highway
Silver Spring, Maryland, 20910, USA

Published
Atmospheric Environment, Vol 28, No. 13, pp. 2197-2210, 1994

Abstract

A Lagrangian model was adapted to simulate the transport, dispersion, and deposition of pollutants from the Kuwait oil fires. Modifications to the model permitted radiative effects of the smoke plume to modify the pollutant's vertical mixing. Calculated SO_2 (sulfur dioxide) air concentrations were compared with the observations from several intensive aircraft measurement campaigns as well as longer-term ground-based measurements. Model sensitivity tests and comparison to the aircraft measurements confirmed: the magnitude of the tabulated emission rates for SO_2 and carbon soot; the most appropriate value for the smoke's specific extinction coefficient was about 4 m^2 g^{-1}; that the model was sensitive to the vertical mixing in the first 100 km downwind from the fires; that the SO_2 conversion rate was about 6% h^{-1}; and although there were large variations in the height of the initial smoke plume and ground-level concentrations were most sensitive to that height, an average value of 1500 m agl (above ground level) provided reasonable model predictions. Six ground-level sampling locations, all along the Arabian Gulf Coast, were used for model evaluation. Although the measurements and model

calculations were in qualitative agreement, the highest space- and time-paired correlation coefficient was only 0.40. The monitoring stations were located in industrial areas, requiring the subtraction of a background concentration of anywhere from 5 to 34 μg m^{-3}, which at some stations was larger than the contribution from the oil fires smoke. The coastal location and lack of correlation between some of the sites suggested that mesoscale flow features not properly represented in the coarse meteorological data used in the computations may have influenced the smoke transport.

Key Word Index: dispersion, modeling, air quality, Arabian Gulf, smoke

1. Introduction

The uncontrolled burning of oil from the Kuwait fields started during February of 1991. Smoke was first visible from satellite images as early as the 9th (WMO Report, 1991) and when ground hostilities started on the 23rd, a substantial portion of the oil fields were on fire. After the cease-fire on the 28th, it took until November of 1991 for all the fires to be extinguished. During this nine month period a substantial number of military and civilians were exposed to various pollutants, smoke, and other combustion products. The human and environmental consequences of these exposures will continue to be evaluated for many years. Initial Arabian Gulf related studies have focused upon summary evaluations from aircraft observation programs (Lawson and Rowley, 1992; WMO Report, 1992; Hobbs and Radke, 1992) and potential climatic feedback scenarios (Small, 1991).

The results presented in this analysis represent an effort to determine if the currently available information about the fires' emissions, chemical characteristics, and the various available measurements are sufficient to use a relatively simple computational approach to evaluate potential smoke plume exposure impacts. Are the available published data internally consistent? Can the emissions inventory in conjunction with reasonable dispersion model assumptions produce concentration estimates that are within the limits of uncertainty of the measured data? To test the various available data and required modeling assumptions, the computational results are compared with measurements of SO_2 (sulfur dioxide) from routine air quality sampling data collected at a variety of locations in Kuwait and Saudi Arabia and aircraft measurements of carbon soot and SO_2.

2. Transport and Dispersion Model

The carbon soot and SO_2 transport and dispersion are calculated by a modified version of the Hybrid Single-Particle Lagrangian Integrated Trajectories (HY-SPLIT) model. The model has evolved through several stages, starting with a simple wind-shear induced particle dispersion study (Draxler

and Taylor, 1982), to which was added air concentration calculations with simple vertical mixing assumptions (Draxler, 1982), and with the further inclusion of the calculation of spatially and temporally varying vertical mixing coefficient profiles and vertical particle motions (Draxler, 1987). Recent modifications include the incorporation of wet sulfur chemistry (Rolph et al., 1992). A recently completed study determined the calculated trajectory accuracy based upon satellite observations of the Kuwait oil fires smoke plume over land (McQueen and Draxler, 1994).

2.1 Base Model Configuration

In HY-SPLIT, advection and diffusion calculations are made in a Lagrangian framework while the meteorological input information is obtained from gridded data fields output from an Eulerian primitive equation model. One pollutant particle represents the initial source. As the dispersion of the particle spreads it into regions of different wind direction or speed, the single particle is divided into several particles to provide a more accurate representation of the effects of the complex flow field. Air concentrations are calculated on a fixed three dimensional grid by integrating all particle masses over a predetermined sampling time. The reference base for the model is described by Draxler (1992). Although the grid spacing of the meteorological grid is relatively coarse, the advection and dispersion calculations are made in a Lagrangian framework, and hence are independent of grid spacing. The concentration calculations and related smoke effects are computed on a high resolution grid nested within the meteorological grid.

2.2 Smoke Feedback Modifications

Several modifications were made to facilitate the computation of air concentrations from pollutants emitted within the Kuwait oil fires' smoke plume. One set of modifications, already incorporated into the model and briefly discussed in the original report (Draxler, 1992, p. 23), permitted the calculation of air concentrations from the simultaneous emission, transport, and dispersion of smoke and additional trace gasses from multiple oil fields.

The dense smoke, especially near the source region, absorbed solar radiation, and inhibited the development of a normal daytime convective boundary layer which would quickly mix the elevated smoke plume to the ground. Because the effects of smoke are not incorporated into any of the routine meteorological analyses fields, HY-SPLIT was modified to permit smoke concentrations to influence the vertical mixing coefficient. The smoke concentration is vertically integrated each time step to obtain an optical depth, which is used to predict the reduction in ground-level temperature due to the absorption of solar radiation by the smoke. A new below-plume ambient temperature profile is then computed and the vertical mixing coefficient is re-calculated. The subsequent transport and dispersion of both the smoke and the trace gas are affected by the new mixing coefficient. The net effect of this process is to inhibit the vertical mixing of smoke to the ground, especially in regions of dense smoke concentration. The mechanism is discussed in greater detail in Appendix A.

For the oil fires simulations, two pollutants, carbon soot and SO_2, were released at the center of each pollutant source field. Both are subject to dry deposition. Wet removal is not considered in this study. The carbon soot particles settle gravitationally, assuming a particle diameter of about 0.8 μm (Cofer et al., 1992). Deposition calculations were made using parameterizations of the a deposition velocity that followed the resistance analogy (Hicks, 1986). However because the bulk of the smoke plume was elevated, the inclusion or exclusion of deposition calculations had little ground-level impact, comparable to the precision of the model calculations. This will be disussed in more detail in section 6.

3. Data Requirements

3.1 Meteorological

The NOAA National Weather Service's National Meteorological Center (NMC) runs a series of computer analyses and forecasts (Petersen and Stackpole, 1989). One of the primary operational systems is the Global Data

Assimilation System (GDAS, Kanamitsu, 1989), which uses the spectral Medium Range Forecast model (MRF - Sela, 1980), to assimilate observations with "first guess" data fields (forecasts from the previous model run) to produce the final "analyzed" data fields.

The 11 x 11 extract of the global MRF analysis fields used for the Arabian Gulf simulations is shown in Fig. 1. The spacing is about 300 km at that latitude and the fields have a vertical resolution limited to the mandatory pressure levels (1000, 850, 700 hPa, etc.). The fields are available every 6 hours with the 0000 and 1200 UTC outputs from the GDAS initialization and the 0600 and 1800 UTC fields derived from the MRF 6-hr forecasts enhanced with any GDAS data available at those times. Prior to any model computations, all the data fields were linearly interpolated at 3-hr intervals. The global MRF fields (TD-6140) are available from the National Climatic Data Center (Asheville, NC).

Atmospheric flow in the Arabian Gulf is strongly driven by the large scale northerly Shamal winds which are persistent from May through September. The MRF horizontal grid spacing is sufficient to resolve the flow on this scale based upon comparisons between calculated trajectories and satellite images (McQueen and Draxler, 1994). During earlier months (February through April) of the study period, smaller scale frontal systems and sea breeze circulations are more frequent and may not be properly resolved by the MRF analysis. However without either the output fields from a mesocale model simulation (beyond the scope of this study) or more spatially detailed observations (not available), these uncertainties will be inherent in any of the unaveraged shorter term model calculation results.

3.2 Emissions

Emissions from individual wells were clustered into 8 separate oil fields (Fig. 2). Each field cluster was assigned a center position and radius (Table 1) that would approximate the areal coverage of the fires from the wells in that field. The number of burning wells and total oil flow in each field are available (Al-Besharah, 1991; Robinson, 1992) for each week from

March 16, 1991 through November 16, 1991. The emission rate from the first week tabulated was used for the two weeks prior to that date. The oil flow rates were used to compute the SO_2 and carbon soot emissions based on conversion factors (Table 1) given by Laursen et al. (1992) for oil fields either north and south of Kuwait City. The emission rate for SO_2 and soot was calculated each week of the computational period and was assumed to be constant for that week. Emissions for the period are summarized in Fig. 3. The total emissions are dominated by the fields to the south of Kuwait City.

The initial plume height at all fields for all pollutants was set to a constant mid-point of 1500 m for the entire simulation period with the pollutant material initially distributed uniformly through a layer from about 1100 to 1900 m above ground. The release height and vertical distribution near the source is consistent with limited observations by Hobbs and Radke (1992), Daum et al. (1993), Johnson et al. (1991), and Browning et al. (1992). A similar initial plume height was inferred from a modeling study by McQueen and Draxler (1994), although substantial daily variations were found. Additional discussion on the initial release height is in section 4.3. Although the initial release height was a constant, internal model calculations used a downwind plume height value that was based upon the calculated soot concentration centroid height, which could vary in response to changing meteorological conditions.

4. Model Evaluation using Aircraft Measurements

The primary evaluation of the model's internal assumptions was performed by comparing the results to measurements of soot and SO_2 from three different aircraft sampling programs that were available at the time of this analysis.

4.1 Data Analysis Procedures

Aircraft from various countries were operating in the Gulf region for intensive measurements of the oil fires smoke plume for brief periods during March, May, June and August, 1991. The WMO report (1992) describes each

aircraft mission in detail. Data from three aircraft (Table 2) were available from the KUwait Data Archive (KUDA - Haggerty, 1992): SO_2 measurements by the U.S. Department of Energy (DOE) Gulf Stream I, the German Ministry of Environmental Protection (GMEP) Piper, and the National Center of Atmospheric Research (NCAR) Electra aircraft. At the time this study was conducted, soot measurements were only available from the GMEP aircraft from the KUDA.

All aircraft measurements were analyzed from the original KUDA 10 s sampling frequency data files by combining them at one minute frequencies and averaging along each flight transect. The flight transects normally crossed the plume at directions perpendicular to the wind at various heights and lasted about 10 min. Table 3 lists the aircraft flight dates and times used in the model evaluation. Not all flights were used due to errors in the data or because the smoke plume was never sampled during the flight.

Once SO_2 and soot were averaged for each flight transect, the air concentrations were grouped by downwind distance and height every 50 km downwind and every 500 m in height. All grouped data were averaged. This procedure was employed primarily to reduce the measurement "noise" introduced by meteorological variability in combination with the relatively infrequent aircraft sampling and to convert the measurements into a spatially smoother data set more consistent with the output from a continuous model calculation.

Model concentrations were also calculated at 500 m intervals through a 4 km layer over sequential 6 h averages. Aircraft sampling missions tended to have a duration of several hours (see Table 3) and therefore the 6 h period nearest in time to the operational period was used in the comparison. An analysis program was designed to produce a plume cross-section by computing the average pollutant concentration along a typical 80 km aircraft transect, orthogonal to the plume centerline at each downwind distance and vertical layer. Measurements and model calculations were only paired in time as differences in plume positions were not taken into account. The primary objective of the aircraft sampling was to measure plume composition and to quantify the smoke plume properties.

4.2 Carbon Soot Results

The GMEP aircraft carbon soot measurements allow tests of some of the primary assumptions of the radiative feedback portions of the model. The first set of tests was to determine the sensitivity to the resolution of the model concentration grid. The model was run with grid factors (ratio of the fixed meteorological grid size to that of a variable concentration grid) of 10, 20, and 40, which results in a concentration grid spacing of about 30, 15, and 7 km, respectively, at the latitudes in the Gulf region. The model results and measurements for soot are shown in Fig. 4.

As the grid becomes more coarse, the region of highest concentration moves farther downwind due to the intersection of the near-source region plumes with the more widely spaced grid points farther away from the source region. The model forces a plume to impact at least one concentration grid point each time step. At a finer grid resolution there may be several grid points between the source region plume and the first aircraft sampling distance averaging bin (50 km).

Although the highest grid resolution simulation showed the best results, even finer resolution runs are not practical because the internal structure of the code does not permit plume positions to be resolved smaller than 0.01 of the resolution of the meteorological grid, or about 3 km. Hence it is possible that even the 7 km concentration grid might lead to aliasing of calculation results. The 7 km grid also results in huge output files and suggests a computational resolution not consistent with the coarser grid input data driving the advection calculations. Therefore subsequent calculations were performed with a grid resolution of 15 km.

These results also provide an estimate of the minimum calculational precision of the model due to the concentration grid resolution. There are other contributions that degrade model precision and contribute to the uncertainty, typically from the integration method and dispersion parameterizations. However those are beyond the scope of this investigation. Excluding the 50 km distance and 30 km grid simulation, variations in the

model concentration calculations appear to be on the order of 10 to 20%.

Fig. 4 also shows that the gross carbon soot concentration calculations, at the farther downwind distances, are very consistent with the measurements. The model calculations are, of course in addition to many of the assumptions within the model, primarily a function of the tabulated soot emission factors, further supporting the magnitude of the tabulated values.

Another uncertainty was the value of the specific optical extinction coefficient for smoke. Previously quoted researchers found values ranging from 1 to 12 $m^2\ g^{-1}$ (Appendix A). Model calculated results of optical depth and surface cooling versus downwind distance are shown in Fig. 5 for two different extinction coefficients. Aircraft measurements summarized in Table A.1 (Appendix A), show measured optical depths ranging from 0.5 to 2 and with concomitant ground-surface cooling from 2 to 8 degrees Celsius, a result more consistent with an extinction coefficient of 4 $m^2\ g^{-1}$, the value which will be used in all subsequent calculations.

The effect of the smoke is propagated through the model in the calculation of dispersion of the smoke and other pollutants through modification of the below-smoke-plume temperature profile and resulting vertical mixing coefficient. Although the mixing is adjusted at all model levels within the smoke plume, the effect is shown in Fig. 6 as the average vertical mixing coefficient in only the lowest layer of the model, with and without adjustment for the effects of soot. Note that the largest differences occur within the first 100 km, when the smoke concentrations are the greatest. The reduced mixing coefficient results in much less smoke and other pollutants mixing down toward the ground near the fires' source. One interesting feature is that the unadjusted mixing coefficient near the source is much larger than the coefficients farther downwind. This is a result of a combination of coarse meteorological grid resolution and the persistent orientation of the downwind smoke plume over the Arabian Gulf. Examination of Fig. 1 illustrates that the two nearest grid points to Kuwait are both over land, while three of the four downwind grid points are either over water or on the land-water interface. Therefore there was consistently greater surface heating and

vertical mixing represented by the coarse grid data near Kuwait than farther downwind.

4.3 SO_2 Results

All three aircraft made measurements of SO_2. The GMEP and NCAR missions occurred about the same time around the end of May 1991 and the DOE mission two months later during early August. In addition, as will be discussed in the next section, SO_2 was the only routinely measured pollutant at ground-level, before, during, and after the oil fires. SO_2 is not an ideal verification tracer, because of the uncertainty regarding emission factors as well as any conversion or other removal processes that might affect the air concentration. These factors must be taken into account when using SO_2 as a tracer for model evaluation.

Studies by Ferek et al. (1992) reported conversion rates of SO_2 to sulfate to be about 6% h^{-1}, a value comparable to that reported by other investigators (Busness et al., 1992; Daum et al., 1993; Cofer et al., 1992; Jenkins et al., 1992; Luke at al., 1992). The conversion rate assumption was tested by comparing the aircraft measurements to the model calculations, using four different SO_2 conversion rates, shown in Figs. 7, 8, and 9, for the three aircraft. The solid line on each figure represents a power function least-squares regression line through the measured data points which represent the average from all the flights. The averaging procedure was described in detail in Section 4.1. The flights are listed in Table 3 and the average values shown in each illustration are composed of 62, 64, and 51 individual plume transects, for the GMEP, NCAR, and DOE aircraft, respectively.

Although the GMEP (Fig. 7) and NCAR (Fig. 8) aircraft operated at about the same time, the GMEP aircraft's SO_2 concentrations were on average about 50% higher than the NCAR measurements, especially at the farther downwind distances beyond 300 km. The DOE (Fig. 9) measurements are somewhat lower than those from NCAR, however they were made two months later, and therefore properly reflect the lower emissions due to the reduction in the number of burning wells between the two periods. Adjusting for the reduced emissions,

the NCAR and DOE SO_2 concentration magnitudes are the most comparable.

It is difficult to pick the best conversion rate to use from these illustrations with any degree of precision. Figs. 7-9 show that a 2% change in the hourly conversion rate results in a 20% to 25% change in downwind concentration, comparable to the variation between adjacent measurement points. Subsequent model calculations will use the same rate during the daytime and nighttime hours. It is possible that the conversion rates are lower at night, however all the flights occurred during daylight hours (see Table 3). The majority of the DOE and NCAR flights started in the morning while GMEP flights started in the afternoon. If there was a strong diurnal variation in conversion rates, the GMEP flights should have measured lower concentrations. However as noted previously, GMEP SO_2 concentrations are higher than those measured by the NCAR aircraft. These results would also be modified by the "age" of the plume that is being sampled. In consideration of the uncertainties stated, the measurements shown in Figs. 8 and 9 between NCAR and DOE appear to be the most internally consistent, and those regression slopes more nearly follow the slope of the calculations using the 6% h^{-1}, especially farther downwind. This value is within the range quoted by other investigators and will be used in the subsequent comparison of ground-level SO_2 concentrations. Computationally the conversion rate is handled like a decay term with a half-life ($T_{½}$) of 0.47 days such that the pollutant mass is reduced each time step by $e^{-?t\ß}$, and where $ß = - \ln 0.5 / T_{½}$.

The concentration calculations (Figs. 8 and 9) for the different conversion rates range over a factor of two in concentration and bracket a majority of the measured data points. This is probably sufficient to suggest that the SO_2 emission factors are correct to within this same range, given all the cumulative uncertainties represented by the data in these diagrams.

Several previous studies (Hobbs and Radke, 1992; Daum et al., 1993) alluded to the complex vertical structure of the smoke plume, perhaps inconsistent with the modeling approach of using a constant release height of 1500 m. As an illustration, the averaged NCAR SO_2 measurements are shown in

Fig. 10 by release height and distance. Note that the highest concentrations near the source region are located at heights of about 1500 m, however considerable material is also evident at other heights. The model results, shown in Fig. 11, do not show the same vertical complexity, but the magnitude and vertical depth of the primary plume concentration matches the measured data. Some of these differences may be due to using a constant release height in the calculations during the entire period as there could have been large day to day variations in the initial plume rise height. Further it is not possible to determine if the complexity illustrated in the measurements truly reflects the conditions as averaged over the many sampling days or simply arises from insufficient sampling frequency. In any case the 1500 m initial height seems to capture the bulk of the release material. The results from the other aircraft were comparable. The release height factor will be discussed again in section 6.

5. Model Evaluation using Ground-Level Measurements

There were a variety of continuous monitoring air quality sites located in the area. We selected a subset of these based upon a variety of quality control measures and duration of record. The locations of the sites used in the subsequent discussion are shown in Fig. 12. Table 4 summarizes the data availability for these sampling sites.

5.1 Ground-Level Measurements and Calculations

One complication of the ground-level data was that they were taken at routine air quality monitoring sites, usually near local industrial sources. Therefore the data contain an ambient background value that reflects other emissions in addition to any contribution added by the oil fires. An attempt was made to remove this local "background" at each of the sampling locations by estimating the background at each site, which is then subtracted from the higher measured concentrations. A cumulative concentration plot is shown in

Fig. 13 for each station. If the concentration distributions reflected constant ambient background, they would be flat, then slope rapidly upward, indicating concentrations clearly above background. Although we have no information about the analysis methods, precision, or accuracy, of the ground-level data, analysis uncertainty is typically reflected by increases in slopes at the lower concentration levels. With the exception of the Mansouriya site there is no clear break in the distribution between background and plume concentrations, suggesting that the median value could be an appropriate definition of ambient background. The Mansouriya background is much lower than the others; perhaps because of a conflict-induced reduction in industrial activity. The background SO_2 concentrations (Table 5) are therefore defined as the 50th percentile values from the cumulative concentration probability distributions (Fig. 13) computed from the available data between January and August of 1991 (Table 4).

The question of how well this background value partitions the contribution from local sources versus the more distant oil fires contribution can be addressed by examining the concentration time series available prior to the fires' start. For instance at Abqaiq the median value of 21 is shown with the concentration time series at that site in Fig. 14. The data on the plot support the assumption of a generally constant background over the 6 month period of January through June, 1991; the oil fires' smoke did not apparently alter the ambient SO_2 levels. Prior to the fires' start, few events exceeded the background. However there is a significantly greater number of high concentration events that occur starting in late February, after the fires had begun. Time series plots for the other sites are similar. Therefore one conclusion is that the fires did not raise the "background" levels as much as they increased the number of high events due to intermittent plume impactions at a given site.

A dataset for comparison with SO_2 calculations was generated by first subtracting the background from the ground-level measurements, with measurements less than background set to zero. Setting below-background values to zero does not bias the magnitude nor number of plume events. The background-subtraction is primarily a visual tool, as the model will only

predict concentrations due to smoke plume events. The resulting values were then smoothed temporally. Weekly running averages were computed to reduce the day-to-day variability. To retain as many observations as possible, six-day averages were permitted, as opposed to a weekly, or seven-day average, when individual daily data were missing. The averaging acts like a low-pass filter and thereby removes some of the higher frequency measurement fluctuations that the model, due to the coarse temporal and spatial resolution, has little possibility of simulating.

As seen in Fig. 12, four (Rahimah, Damman, Dhahran, and Abqaiq) of the six sampling sites are clustered together at the most distant range. If the variance in the concentration measurements from the oil fires smoke is due entirely to larger scale synoptic meteorological conditions, one would expect that the correlations between stations should be very high. At these distances one would expect the oil fires' smoke plume to have comparable impacts on these stations, however when weekly cross-correlation coefficients were computed for the measured sampling data, Dhahran had the highest correlation (0.89) with nearby Damman, while Rahimah was uncorrelated with any other site. The cross-correlations were about the same when computed with and without the background subtracted from the measurements. Lower correlations at some stations suggest that the variance is driven by other processes, which could be anything from local emissions to mesoscale effects from the seabreeze. In the subsequent discussion three stations were selected for analysis, one for each distance range: Monsouryia (near), Tanajib (mid-range), and Dhahran (far). The analysis was then composed of weekly concentrations for the three ground-level sites.

Daily average (9 am - 9 am) air concentration model calculations were made for the entire period at each of the sites. The model calculation outputs were then averaged in a manner comparable to the measurements.

5.2 Time-Series Results

The weekly time series plots at the three ground-level sampling sites are shown in Figs. 15-17. The dashed lines represent the subtracted

background value at each sampling location. A concentration comparable to the dashed line is at twice ambient background. Any biases in these figures is only a result of the background subtraction, clearly indicated on each figure, and the model concentration calculation.

The weekly time series plot at Mansouriya, shown in Fig. 15, has only one significant measured plume (high concentration) event (near Day 105). Although background levels have been subtracted, plumes of about 5 μg m^{-3} are twice ambient background. At Mansouryia there was no significant correlation between measured and calculated values and such a comparison is essentially meaningless in this situation due to the large number of low measured plume values. In that region the wind was usually from the north, and with the site to the north of the southern fields, from which most of the smoke was produced, few major plume events were expected. Further, the smoke plumes rarely impacted the ground near the fires due to the thermal effect of the fires and in combination with the low-level atmospheric stability introduced by the radiative effects of the smoke. With the exception of a few periods in which the model predicted events that were not observed, some of which had missing data, the one encouraging feature is that the model calculations were as low as the measurements.

The comparison at the mid-downwind site at Tanajib is shown in Fig. 16. There are many more significant plume events occurring at this site and there are more calculated than measured events. Note also the longer duration of the variations in the measured high concentrations. The model calculations appear to have a distinctive period of plume events lasting 10 to 15 days, however a similar periodicity is not as evident in the measurements. This is perhaps due to the local or mesoscale processes confining the plume within the coastal region while the calculated plume was more subjected to synoptic waves suppressed in that local regime. The model does calculate peaks and troughs comparable in magnitude to the measurements. Again there was no significant correlation between measurements and calculations.

The situation at Dhahran (Fig. 17) is somewhat more complex due to the lower measured plume values than at Tanajib. The model calculations do

capture the overall long-term trend and some of the peaks and troughs. The calculations show a similar structure to those at Tanajib, a similar periodicity and with more frequent calculated peak values. However unlike Tanajib the values are closer to ambient background, which diminishes the significance of the results, although the correlation was the highest of any station at 0.40.

Although the level of skill of the model in predicting the variations of concentration was marginal, the model correctly predicted SO_2 plume magnitudes and the approximate concentration trends between the near, mid, and distant sampler. Very few of the measured or calculated concentrations ever exceeded twice ambient background. Considering the uncertainties in the emissions, transformation, and sampling (unknown local sources), the ground-level sampling results suggest that the overall effect of the oil fires' smoke had little effect on local air quality farther downwind. The elevation of the smoke plume and initial inhibited mixing to the ground resulted in the ground-level concentrations at first increasing and then decreasing with distance. The near source station, Mansouryia, had the lowest concentrations, while Tanajib, the mid-distant site, had the highest concentrations. Concentration values again dropped off at Dhahran, the most distant sampler. The model performance with regard to the concentration magnitudes suggests the SO_2 emission factors as well as conversion rates were estimated reasonably accurately.

6. Sensitivity Test Summary

The model and computational approach outlined in the previous sections contain many assumptions, some explicitly stated and others perhaps more obscure. However each will produce a different response over the range of controlling paramameters. Therefore several additional model sensitivity simulations were conducted to examine the model response in terms of calculating ground-level SO_2 concentrations. There will be no reference to any of the measurements as the primary interest is a comparison of the relative importance of various model assumptions and paramterizations.

It was noted earlier in section 4.2 that a factor of two change in concentration grid resolution results in a 10 to 20% change in calculated concentrations. A particular grid configuration has direct consequences in the computation of air concentrations at specific receptors but also many indirect effects due to the coupling of smoke optical depths and pollutant vertical mixing. Model responses within this range certainly fall within the computational uncertainty of the total model system which would include the additional undocumented effects from the horizontal advection, vertical motion, and dispersion parameterizations.

The most important simulation assumption is the value of the initial release height. Our previous study (McQueen and Draxer, 1994) found that initial plume heights could vary over quite a range (standard deviation of about 800 m) from the average value of 1500 m used in the calculations. Simulations with the initial release at 1000 m showed ground-level concentrations to increase over a factor of two. However when the release height was raised to 2000 m the ground-level concentrations only decreased by about 25%. This suggests that the average plume (1500 m release) was already substantially elevated and had little ground-level impact. That is elevating the plume further did not have as much impact as lowering the plume. Therefore further model improvement, i.e. better correlation with measurements, can be most easily attained by improving estimates of the initial smoke plume heights. The trajectory-error minimization technique developed by McQueen and Draxler (1994) could not be used to determine an initial plume height each day because the coarse vertical resolution of the meteorological analysis fields are insufficient to resolve the wind shears in the lower troposphere.

An elevated plume with little ground-level contact will also not have any significant deposition. A simulation with no deposition showed the ground-level SO_2 concentrations to decrease by about 12 to 25%, which as noted earlier is comparable to the precision of calculation. What is particularly interesting is that the concentrations went down when deposition was turned off. This is a result of the smoke-feedback to the mixing -- denser smoke results in less mixing to the ground. A simulation with the smoke mixing

feedback turned off results in a 20 to 60% concentration increase. Primarily due to the elevated nature of the plume, deposition has little impact upon ground-level concentrations.

Although there is a significant diurnal range in the SO_2 conversion rates over the eastern United States, there have been suggestions (WMO Report, 1992) that the smoke plume chemistry is quite different for the Oil Fires. It is certainly possible that the conversion rates are lower at night as noted previously in section 4.3. One simulation was performed with the nighttime conversion rate at 1% h^{-1} while the daytime rate remained at 6% h^{-1}, and the ground-level concentrations increased by about 50%, a result consistent with the sensitivity shown in Figs. 7-9.

7. Conclusions

A Lagrangian model was modified to simulate the transport and dispersion of smoke and other combustion products from the Kuwait Oil Fires. The model accounted for the effect of the dense smoke plume upon the meteorological dispersion environment by adjusting the vertical mixing coefficient in response to the smoke's soot concentration. The effect of which was to inhibit the vertical mixing of smoke to the ground, especially in regions of dense smoke concentration. Internal model computations of the vertical mixing coefficient suggested that mixing may have been reduced by as much as a factor of three underneath the denser portions of the smoke plume. The model was extensively tested and calibrated with aircraft measurements of carbon soot smoke and SO_2.

The aircraft measurements were used to determine the optimum values for some of the more uncertain model parameters. A smoke specific extinction coefficient of 4 m^2 g^{-1} was found to give the best agreement while the SO_2 measurements suggested using a 6% per hour conversion rate. The overall degree of fit of the majority of the measured data points directly within the smoke plume to the model calculations suggests that the tabulated SO_2 and soot emission factors are reasonably correct. The measurements made at many

different levels and distances found a vertical complexity to the plume structure that could not be reproduced by the model. However it is uncertain if this is due to insufficient sampling frequency or meteorological processes. The model assumption of a constant 1500 m initial plume height generally captured the main plume although model predictions are most sensitive to this assumption.

Ground-level measurements of SO_2 were used to provide a data set for an independent validation. The calculations showed reasonable levels of agreement with the observations considering the limitations of the validation data introduced by having to subtract an ambient background concentration that was comparable to the concentrations due to the oil fires. If the measured levels of SO_2 can be considered a reasonable surrogate for general "air pollution" due to the fires, then background air concentration levels several hundred kilometers downwind only increased by perhaps 50% due to the fires. The complexity of the ground-level data is illustrated by first increasing and then decreasing concentration values with distance from the fires' source. The nearby site had the lowest concentrations while the mid-distant site showed the highest concentrations. Model performance with regard to the concentration magnitudes suggests the SO_2 emission factors as well as conversion rates were properly determined.

8. Acknowledgements

This research was sponsored by the U.S. Army Environmental Hygiene Agency through the Department of the Army Surgeon General's Office.

9. References

Al-Besharah, Jassem, 1991, The Kuwaiti oil fires and oil lakes - facts and numbers, Proceedings of The Environmental and Health Impact of the Kuwaiti oil fires, Birmingham, England, Oct, 17:12-15.

Busness, K.M., A.A. Al-Sunaid, P.H. Daum, J.M. Hales, R.B. Hannigan, M. Mazurek, J.M. Thorp, S.D. Tomich, M.J. Warren, 1992, Pacific Northwest Laboratory Gulfstream I measurements of the Kuwait oil-fire plume July-August, 1991. PNL-8436, Nov. 1992

Browning, K.A., R.J. Allam, S.P. Ballard, R.T.H. Barnes, D.A. Bennetts, R.H. Maryon, P.J. Mason, D.S. McKenna, J.F.B. Mitchell, C.A. Senior, A. Slingo and F.B. Smith, 1992, Environmental effects from burning oil wells in the gulf. Weather, 47, 201-211.

Cofer, W.R., R.J. Stevens, E.L. Winstead, J.P. Pinto, D.I. Sebacher, M.Y. Abdulraheem, M. Al-Sahafi, M.A. Mazurek, R.A. Rasmussen, D.R. Cahoon, J.S. Levine, 1992, Kuwaiti oil fires: compositions of source smoke, J. Geophy. Res., 97, 14521-14525.

Daum, P.H., A. Al-Sunaid, K. M. Busness, J. M. Hales and M. Mazurek, 1993, Studies of the Kuwait oil-fire plume during mid-summer, 1991. J. Geophy. Res., 98, 16,809-16,827.

Draxler, R., 1982: Measuring and modeling the transport and dispersion of Kr-85 1500 km from a point source. Atmos. Environ., 16, 2763-2776.

Draxler, R., 1987: Sensitivity of a trajectory model to the spatial and temporal resolution of the meteorological data during CAPTEX. J. Clim. Appl. Meteorol., 26, 1577-1588.

Draxler, R., and A.D. Taylor, 1982: Horizontal dispersion parameters for long-range transport modeling. J. Appl. Meteorol., 21, 367-372.

Draxler, R., 1992: Hybrid single-particle Lagrangian integrated trajectories (HY-SPLIT): Version 3.0 -- user's guide and model description, NOAA Technical Memo ERL ARL-195, June, National Technical Information Service, Springfield VA.

Ferek, R.J., P.V. Hobbs, J.A. Herring, K.K. Laursen, R.E. Weiss, R.A. Rasmussen, 1992, Chemical composition of emissions from the Kuwait oil fires, J. Geophy. Res, 97, 14483-14489.

Haggerty, J., 1992, Kuwait Data Archive (KUDA) Version 1.0 User's Manual, National Center For Atmospheric Research. 33pp

Hicks, B.B., 1986, Differences in wet and dry particle deposition parameters between North America and Europe, in Aerosols: Research, Risk Assessment, and Control Strategies, Lewis Publishers, Chelsea, MI, pp 973-982.

Hobbs, P.V. and L.F. Radke, 1992, Airborne studies of the smoke from the Kuwait oil fires. Science, 256, 987-991.

Jenkins, G.J., D.W. Johnson, D.S. McKenna and R.W. Saunders, 1992, Aircraft measurements of the Gulf smoke plume. Weather, 47, 212-219.

Johnson, D.W., C.G. Kilsby, D.S. McKenna, R.W. Saunders, G.J. Jenkins, F.B. Smith and J.S Foot, 1991, Airborne observations of the physical and chemical characteristics of the Kuwait oil smoke plume. Nature, 353, 617.

Kanamitsu, M., 1989: Description of the NMC Global Data Assimilation and Forecast System, Weather and Forecasting, 4, 335-342.

Lawson, J. B. and M. G. Rowley, 1992: Meteorological support for Operation GRANBY. Weather, 47, 183-196.

Laursen, K.K., R.J. Ferek, P.V. Hobbs, R.A. Rasmussen, 1992, Emission factors for particles, elemental carbon, and trace gases from the Kuwait oil fires, J. Geophy. Res., 97, 14491-14497.

Luke, W.T., G.L. Kok, R.D. Schillawski, P.R. Zimmerman, J.P. Greenberg and M. Kadavanich, 1992, Trace gas measurements in the Kuwait oil fire smoke plume. J. Geophy. Res, 97, 14499-14506.

McQueen, J.T. and R.R. Draxler, 1994: Evaluation of model back trajectories of the Kuwait oil fires smoke plume using digital satellite data. Atmos. Envir., 28A, In press.

Petersen, R.A. and J.D. Stackpole, 1989, Overview of the NMC production suite, Weather and Forecasting, 4, 313-322.

Phillips, N.A., 1986, Turbulent mixing near the ground for the Nested Grid Model, Office Note 318, National Meteorological Center, National Weather Service, Silver Spring, MD, 19pp.

Pilewskie, P., F.P.J. Valero, 1992, Radiative effects of smoke clouds from the Kuwait oil fires, J. Geophys. Res., 27, 14541-14544.

Robinson, J. Presentation at the second WMO meeting of experts to assess the response to the atmospheric effects of the Kuwait oil field fires, World Meteorological Organization, Geneva, Switzerland 25-29 May, 1992.

Rolph, G.D., R.R. Draxler, and R.G. dePena, 1992, Modeling sulfur concentrations and depositions in the United States during ANATEX, Atm. Environ., 26A, 73-93.

Sela, J.G., 1980: Spectral modeling at the National Meteorological Center, Mon. Wea. Rev., 108, 1279-1292.

Small, R. D., 1991: Environmental impact of fires in Kuwait. Nature, 350, 11-12.

WMO Report, 1991, Report of the WMO meeting of experts on the atmospheric part of the Joint UN response to the Kuwait oil field fires, World Meteorological Organization, Geneva, Switzerland, April 27-30, 1991.

WMO Report, 1992, Report of the second WMO meeting of experts to assess the response to and the atmospheric effects of the Kuwait oil field fires, World Meteorological Organization, Geneva, Switzerland, May 25-29, 1992.

Appendix A - Smoke Feedback Mechanism

Vertical mixing coefficients are defined at the interface between each meteorological layer through the relation (adapted from Phillips, 1986)

$$K_z = \frac{30}{(2+Ri)}, \qquad \textbf{A.1}$$

where the constant 30 $m^2 s^{-1}$ represents the maximum mixing coefficient, and the Richardson number

$$Ri = g \frac{d(\ln \rho)/dz}{(du/dz)^2}, \qquad \textbf{A.2}$$

where g is gravity, T is potential temperature, u is wind speed, and z is the reference height.

At each time step, prior to the advection calculation, the smoke plume optical depth,

$$d = k * \int \rho \, dz, \qquad \textbf{A.3}$$

is computed at each concentration grid node. Here k is the specific extinction coefficient of smoke (4 $m^2 g^{-1}$), ρ is the smoke concentration, and the integral is taken over the depth of the computational domain. Optical depths were limited to a maximum value of 4.0.

The ratio of the amount of solar energy actually reaching the surface of the earth (I) to the maximum available (I_o) is defined as the transmissivity and is related to the optical depth through

$$I/I_o = e^{-d}. \qquad \textbf{A.4}$$

The cooling that occurs at the earth's surface due to a reduction in solar radiation is a complex process which depends upon all the other terms of the energy budget. On a first order similarity basis, if we assume that changes in the shortwave component lead directly to changes in the long-wave component of the energy balance, then one can express that relationship as

$$(T/T_o)^p \% e^{-cd}, \qquad \textbf{A.5}$$

where T is the cooler surface temperature under the smoke plume, T_o is the initial surface temperature outside of the smoke plume, p is the exponent to convert temperature to an equivalent black-body radiative energy, and c is a constant that contains all the other unknown components needed to balance the surface energy budget. The above equation can be rewritten as

$$A = c/p = \frac{- \ln (T/T_o)}{d}, \qquad \textbf{A.6}$$

where the constants c and p have been combined into the single value of A. Some of the aircraft made simultaneous measurements of cooling and optical depth, which can be used to calculate "A". Aircraft sampling results from two downwind distances are summarized in Table A.1. The results suggest that A = 0.013 is a reasonable approximation for most distances.

Table A.1. Smoke Plume Optical Properties

Reference	1	2	3
Downwind (km)	100	500	100 - 200
Optical Depth	2.0	0.50	2.3 - 1.6
Cooling (°C)	8.0	2.0	10 - 2
Constant (A)	0.0135	0.0134	0.0147-0.0042

1 - Hobbs and Radke, 1992

2 - Johnson et al., 1991

3 - Busness et al., 1992; Daum et al., 1993; Browning et al., 1992

Once the surface cooling has been determined at each concentration grid node the vertical temperature profile is adjusted below the plume and the

vertical mixing coefficients are re-calculated as follows: the plume height at each point is determined to be at the plume centroid position

$$Z_p = \frac{k * ? Z\, dz}{d} . \qquad \textbf{A.7}$$

The new temperature profile is then computed at all meteorological levels only during the daytime hours at or below Z_p.

In addition to the surface cooling it is assumed that the air will be warmed at the center plume position due to absorption of the incoming solar energy. At around 100 km from the fires, the plume absorbed 75-85% of the solar radiation and transmitted about 10%. The instantaneous heating rate at this distance was found to be about $1^oC\ h^{-1}$ (Johnson et al. 1991; Hobbs and Radke, 1992; Pilewskie and Valero, 1992). At the nearest downwind distance for which surface cooling values are available (8^oC at 100 km - Table A.1) the warming rate of $1^oC\ h^{-1}$ would yield a total plume warming of about 4^oC. If we assume that this mechanism is valid during daylight hours and proportional to the smoke optical depth that is used to compute the cooling at the surface, then the plume warming for travel times of less than 12 hours can be approximated to be about 50% of the surface cooling.

The change in temperature at each sub-plume level is then

$$?T = ?Z\ (?_n - ?_o) - ?T_0, \qquad \textbf{A.8}$$

where ?Z is the height above the surface, $?_n$ is the slope of new adjusted temperature profile between the surface and plume level, $?_o$ is the old unadjusted slope, and $?T_0$ is the surface cooling. New mixing coefficients are then computed from the relation given earlier (Eq. A.1) to a height 50% greater that the plume centroid height to account for any enhanced mixing due to warming at the plume top. The 50% height increase in the application of Eq. A.1 is representative of about one standard deviation of the initial plume height as determined in an earlier study (McQueen and Draxler, 1994).

Although the meteorological fields are updated every 6 h, the mixing adjustment calculations are done each time step to insure that the mixing profiles correspond with variations in plume position and concentration.

Surface cooling calculations and plume heating calculations are only performed during the daytime. However to account for some of the near-field thermal effects a reduced plume warming (at 50% of the daytime value) is applied during the night-time hours at the top of the smoke plume. The calculation is intended to capture some of the initial combustion-induced warming by increasing the plume top ambient temperature and therefore increasing the vertical mixing out of the top of the plume. The intent was to match some of the initial larger vertical plume dimensions that were evident from the aircraft observations. However this assumption is arbitrary with really no supporting experimental evidence and model sensitivity tests indicated that it had less than a 10% effect on ground-level concentrations.

List of Tables

Table 1. Oil field fires central locations, radius to approximate areal coverage of fires in the field, and the percent of the burning oil mass that was converted to SO_2 and carbon soot as given by Laursen et al. (1992) based upon conversion factors for fields either north or south of Kuwait City.

Field	Latitude (deg N)	Longitude (deg E)	Radius (km)	SO_2 (%)	Soot (%)
Ahmadi (S)	29.00	48.00	3.0	3.4	.55
Bahra (N)	29.70	47.88	0.32	1.8	.37
Burgan (S)	28.93	47.96	3.0	3.4	.55
Magwa (S)	29.10	47.98	6.0	3.4	.55
Minagish (S)	29.03	47.55	5.1	3.4	.55
Raudhatian (N)	29.88	47.73	5.9	1.8	.37
Sabriyah (N)	29.80	47.85	5.5	1.8	.37
Umm Gudair (S)	28.85	47.72	6.9	3.4	.55

N / S - north or south of Kuwait City

Table 2. Overview of aircraft missions (DOE - Department of Energy, GMEP - German Ministry of Environmental Protection, NCAR - National Center of Atmospheric Research) used for model evaluation as available from the KUwait Data Archive (KUDA - Haggerty, 1992).

	DOE	GMEP	NCAR
Platform	Gulf Stream I	Piper PA31	Lockheed Electra
Positioning	GPS, Height	GPS, Pressure	GPS, Height
Species	SO_2	SO_2, Carbon Soot	SO_2
Instrument	TECO-43S	Flourescence Light Transmission	TECO-43A
Dates	30 July to 17 August	20 May to 6 June	19 May to 4 June

Table 3. Flights used for aircraft analysis and model evaluation by aircraft and date in UTC starting and ending times.

DOE	GMEP	NCAR
Aug 2 03:15 - 07:30	May 20 14:30 - 16:05	May 21 08:15 - 14:34
Aug 4 07:00 - 11:00	May 21 14:40 - 15:45	May 22 08:19 - 13:24
Aug 6 04:50 - 09:30	May 22 13:50 - 17:15	May 29 08:00 - 13:52
Aug 7 05:00 - 09:30	May 26 16:10 - 19:00	May 30 04:55 - 10:59
Aug 11 05:00 - 07:00	May 27 10:45 - 13:00	May 31 06:28 - 09:22
Aug 12 15:00 - 16:30	May 29 9:15 - 11:30	Jun 1 08:08 - 14:03
Aug 13 05:00 - 09:20	May 30 17:35 - 20:00	Jun 2 05:07 - 10:47
Aug 14 05:10 - 09:10	Jun 1 10:40 - 12:00	Jun 4 06:19 - 15:00
Aug 15 07:00 - 11:40	Jun 2 16:45 - 17:40	
Aug 16 07:30 - 11:40	Jun 4 15:50 - 18:20	
Aug 17 07:30 - 11:00	Jun 5 11:30 - 13:00	
	Jun 6 11:20 - 13:00	

Table 4. January - August, 1991 surface SO_2 data availability for selected stations in Kuwait (K) and Saudi Arabia (SA). "X" indicates data are available for the entire month (less than 5 days missing). "---" indicates data are available for only part of the month.

SITE	LAT	LON	JAN	FEB	MAR	APR	MAY	JUN	JUL	AUG
Mansouriya, K[+]	29.3	48.0				X	X	X		X
Tanajib, SA[*]	27.9	48.8				X	X	X		
Rahimah, SA[*]	26.8	50.0	X	X	X	X	X	X		
Damman, SA[º]	26.4	50.1				---	---	---	---	---
Dhahran, SA[*]	26.3	50.1	X	X	X	X	X	X		
Abqaiq, SA[*]	25.9	49.8	X	X	X	X	X	X		

Data source: [+]KEPD = Kuwait Environmental Protection Department, [º]MEPA = Meteorological and Environmental Protection Agency of Saudi Arabia, available from the Kuwait Data Archive (Haggerty, et al., 1992), [*]Saudi Arabian Oil Company (Saudi ARAMCO).

Table 5. Background ground-level SO_2 concentration.

Site / Concentration ($\mu g/m^3$)					
Abqaiq	Damman	Dhahran	Rahimah	Tanajib	Mansouriya
21	30	34	22	26	5

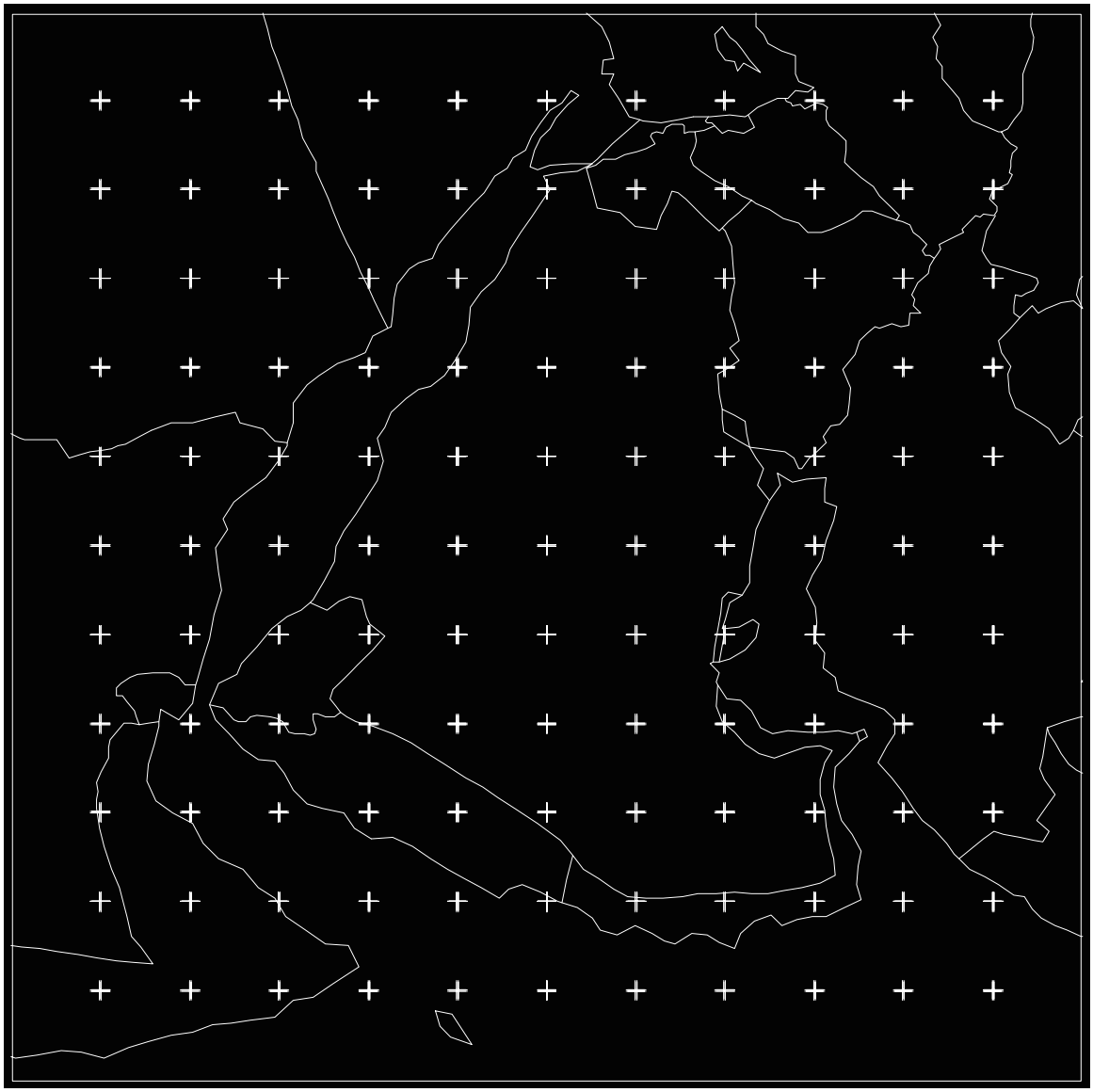

Figure 1. Meteorological sub-grid from the NMC MRF final analysis which was used for the Kuwait oil fires computational domain.

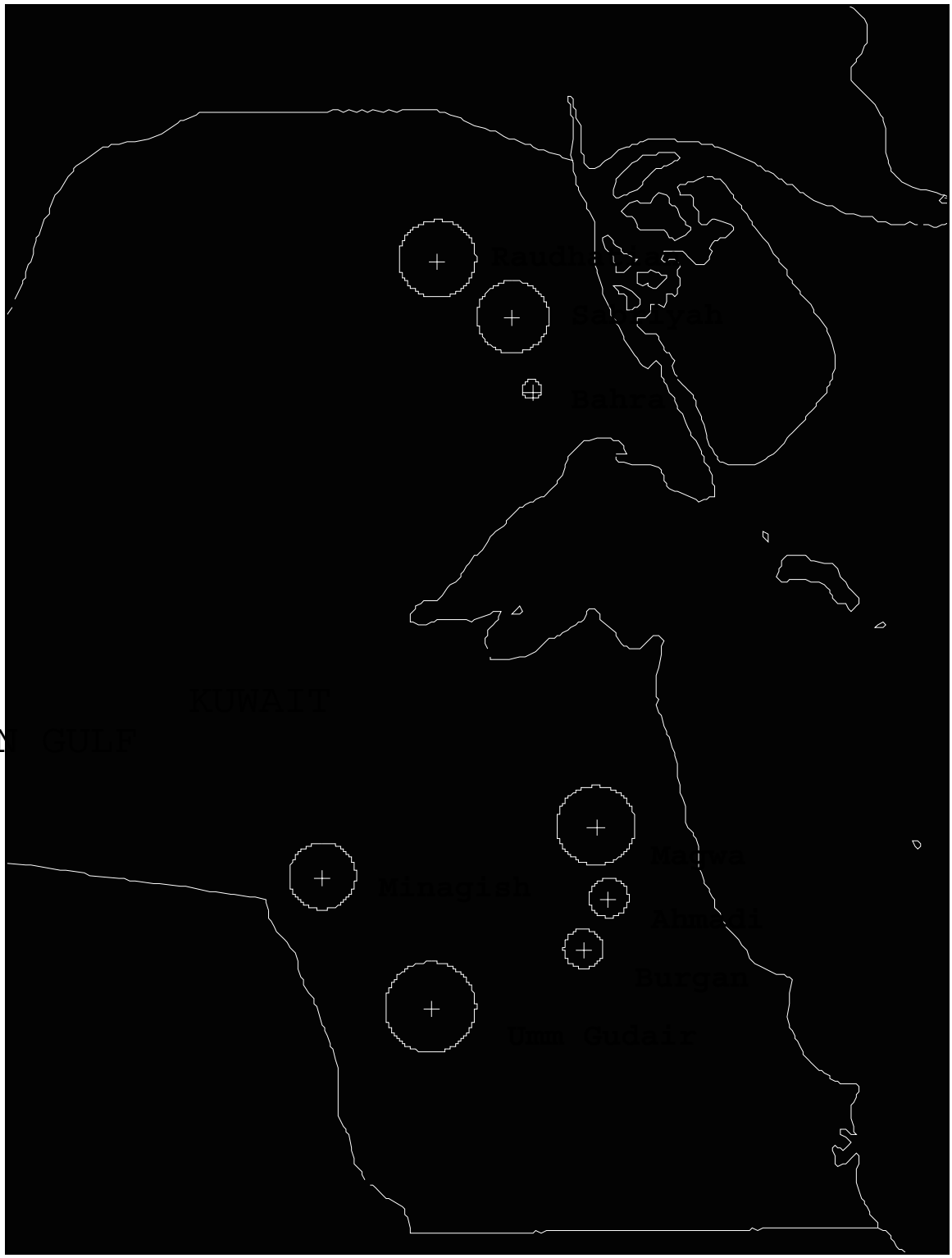

Figure 2. Oil field emission clusters showing area (within circles) assumed to have uniform emissions.

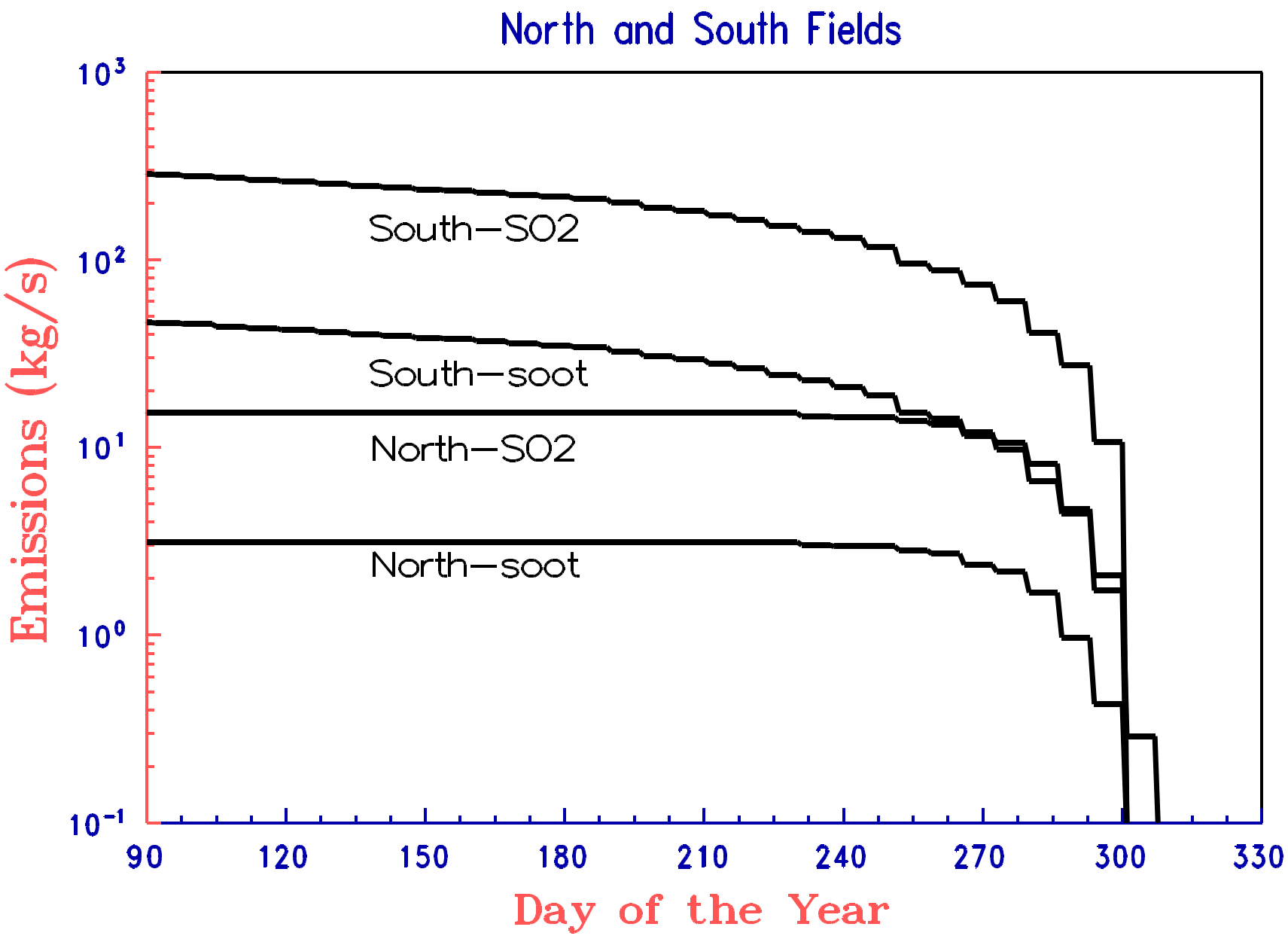

Figure 3. Weekly carbon soot and sulfur dioxide emissions for the northern and southern fields.

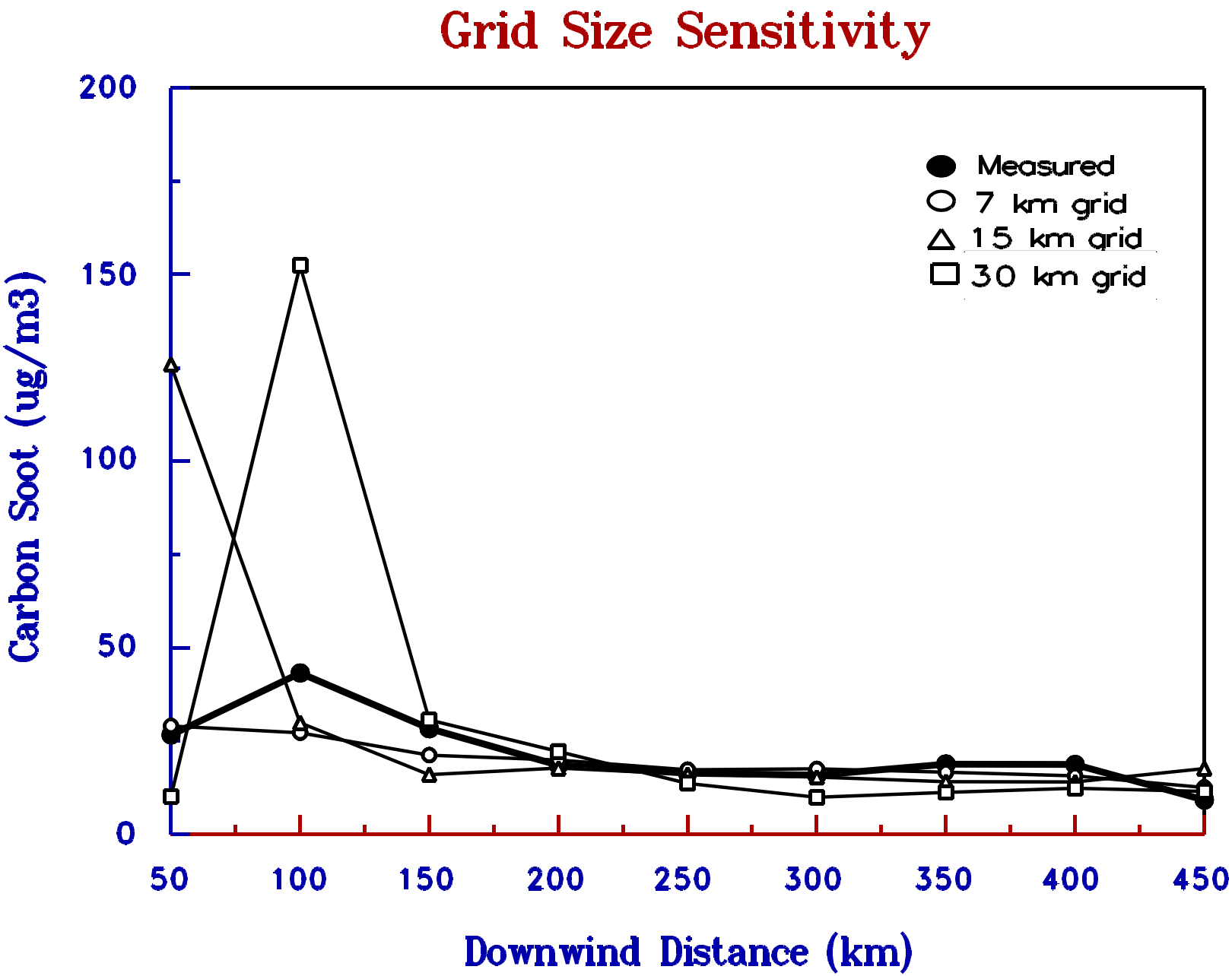

Figure 4. Carbon soot measurements and model calculations in order to evaluate concentration grid size sensitivity.

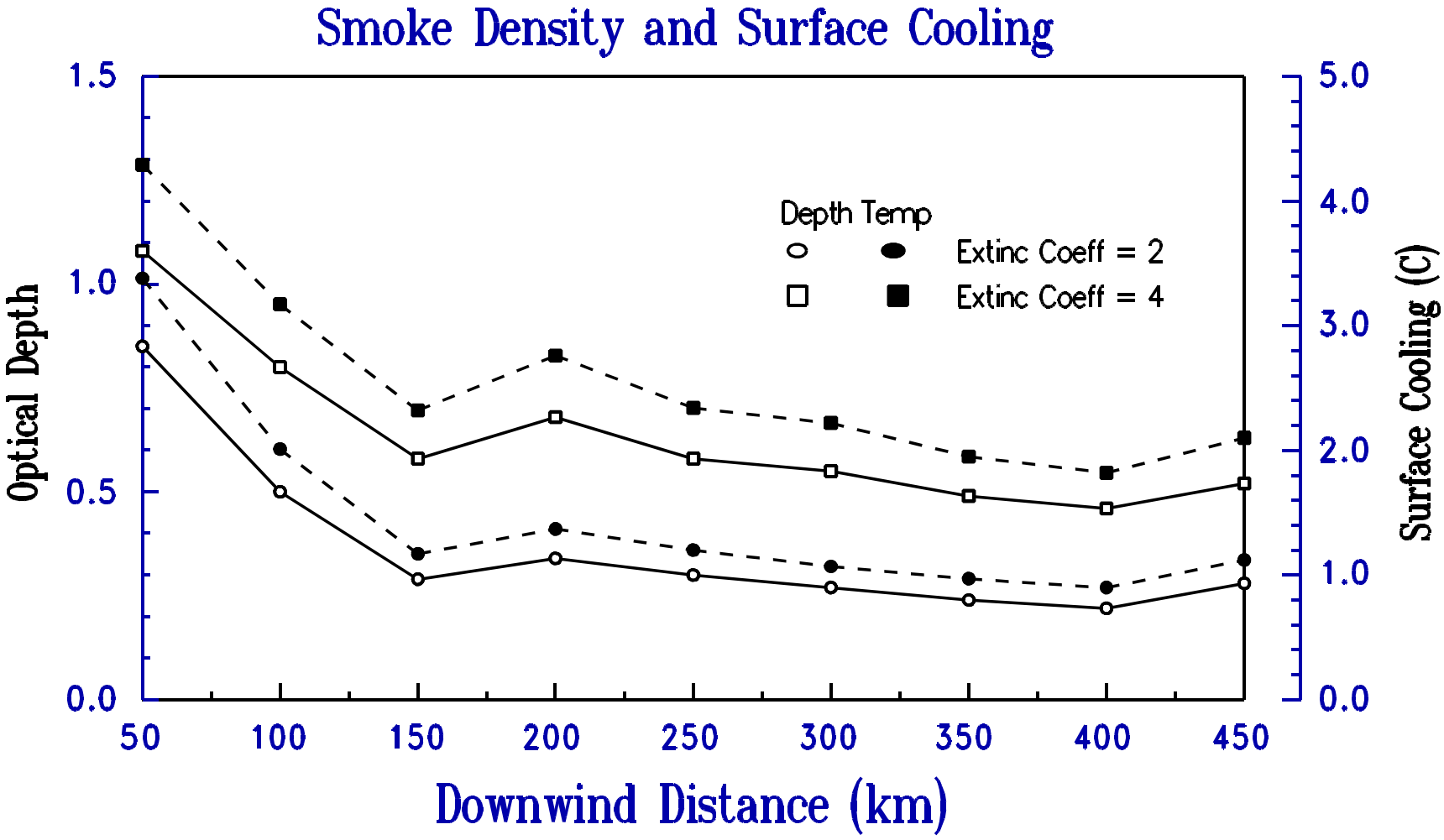

Figure 5. Model calculations of surface cooling and optical depth using different smoke extinction coefficients (2 and 4 m^2 g^{-1}).

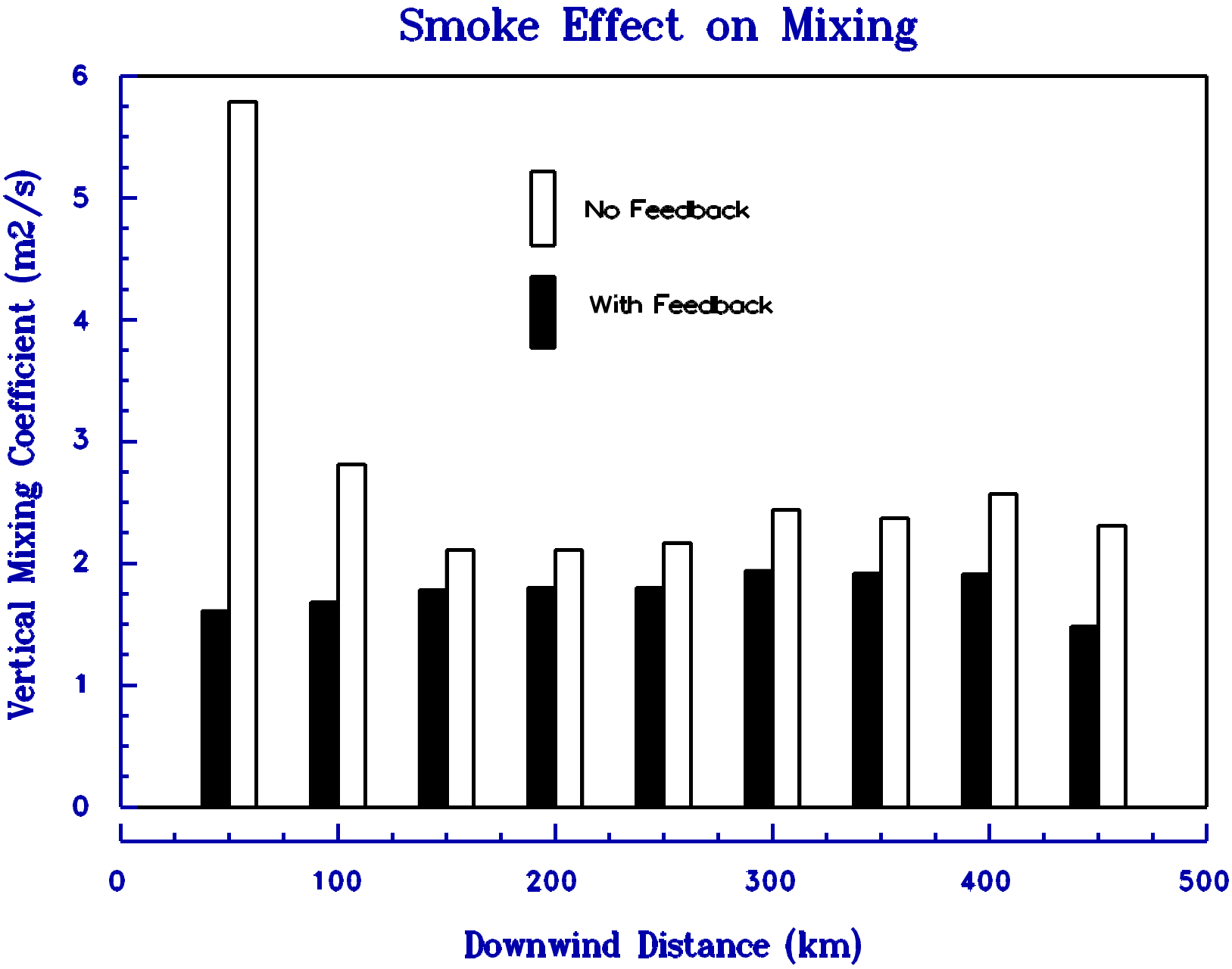

Figure 6. Model calculation of internal vertical mixing coefficients with and without the smoke feedback effect.

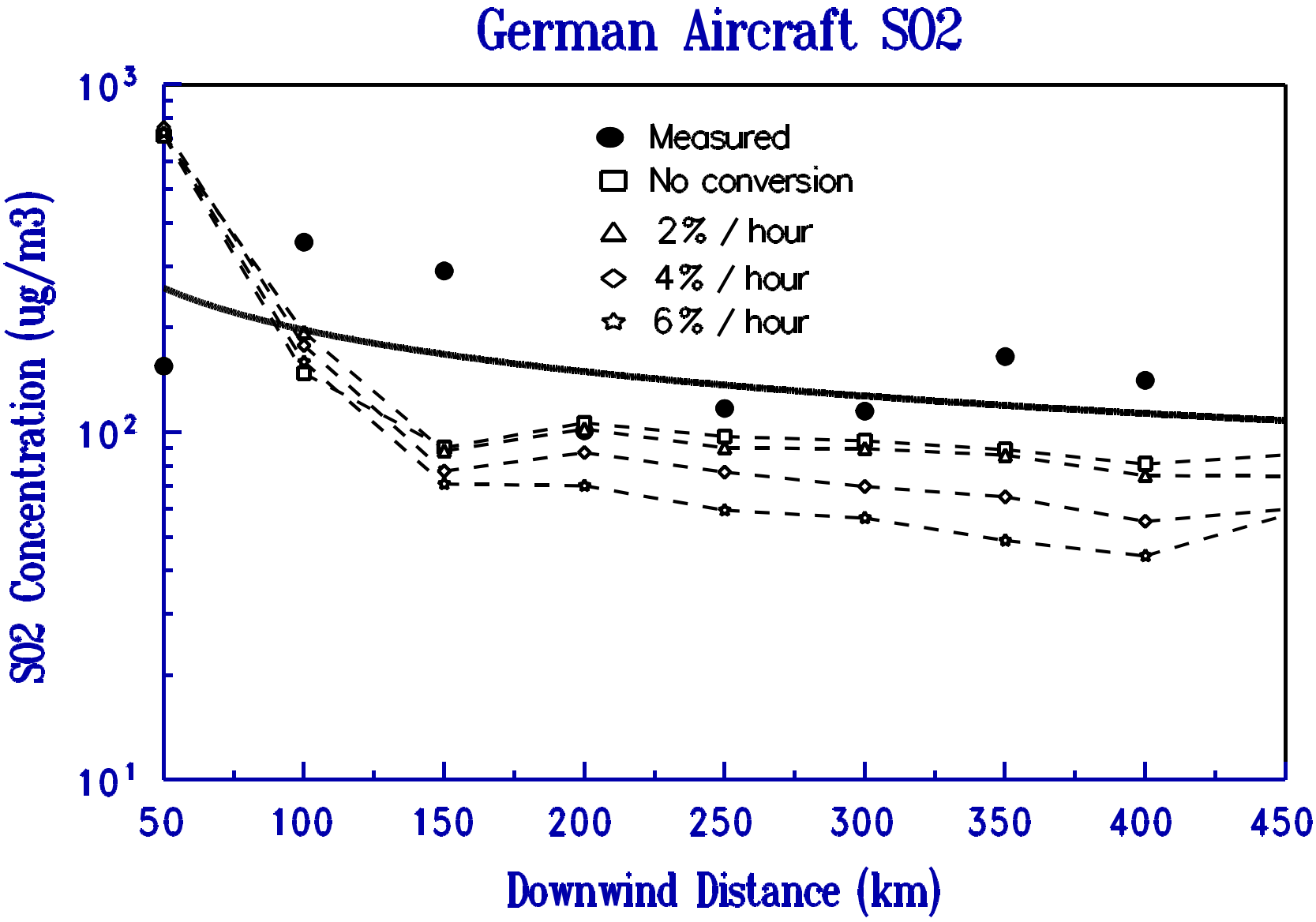

Figure 7. German aircraft SO_2 measurements represented by a power function least-squares fit (solid line) and model calculations using different conversion rates.

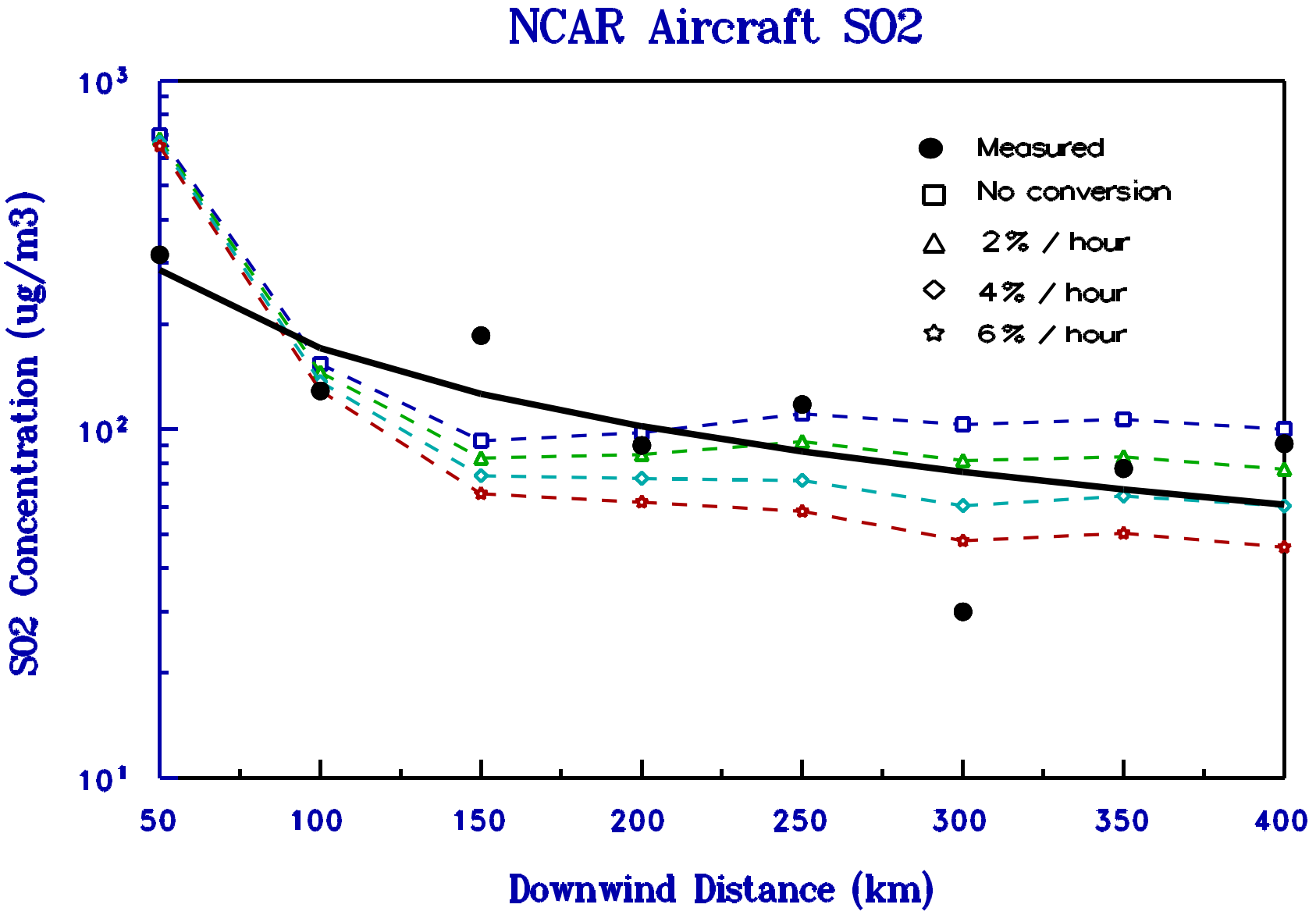

Figure 8. As in Fig. 7, except the solid line represents the NCAR aircraft measurements. Model calculations correspond to the same time periods as the measurements.

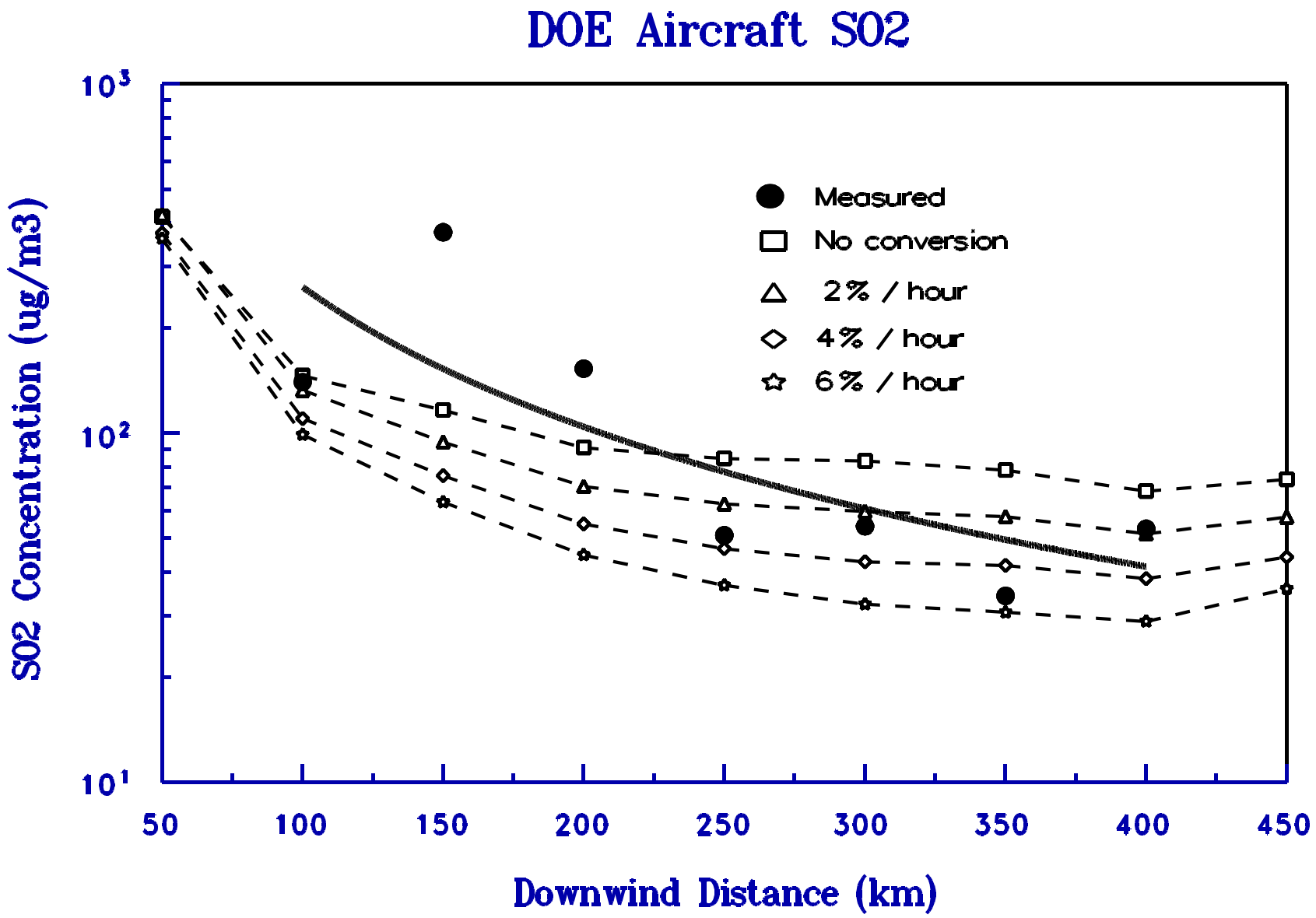

Figure 9. As in Fig. 8, except the solid line represents the DOE aircraft measurements.

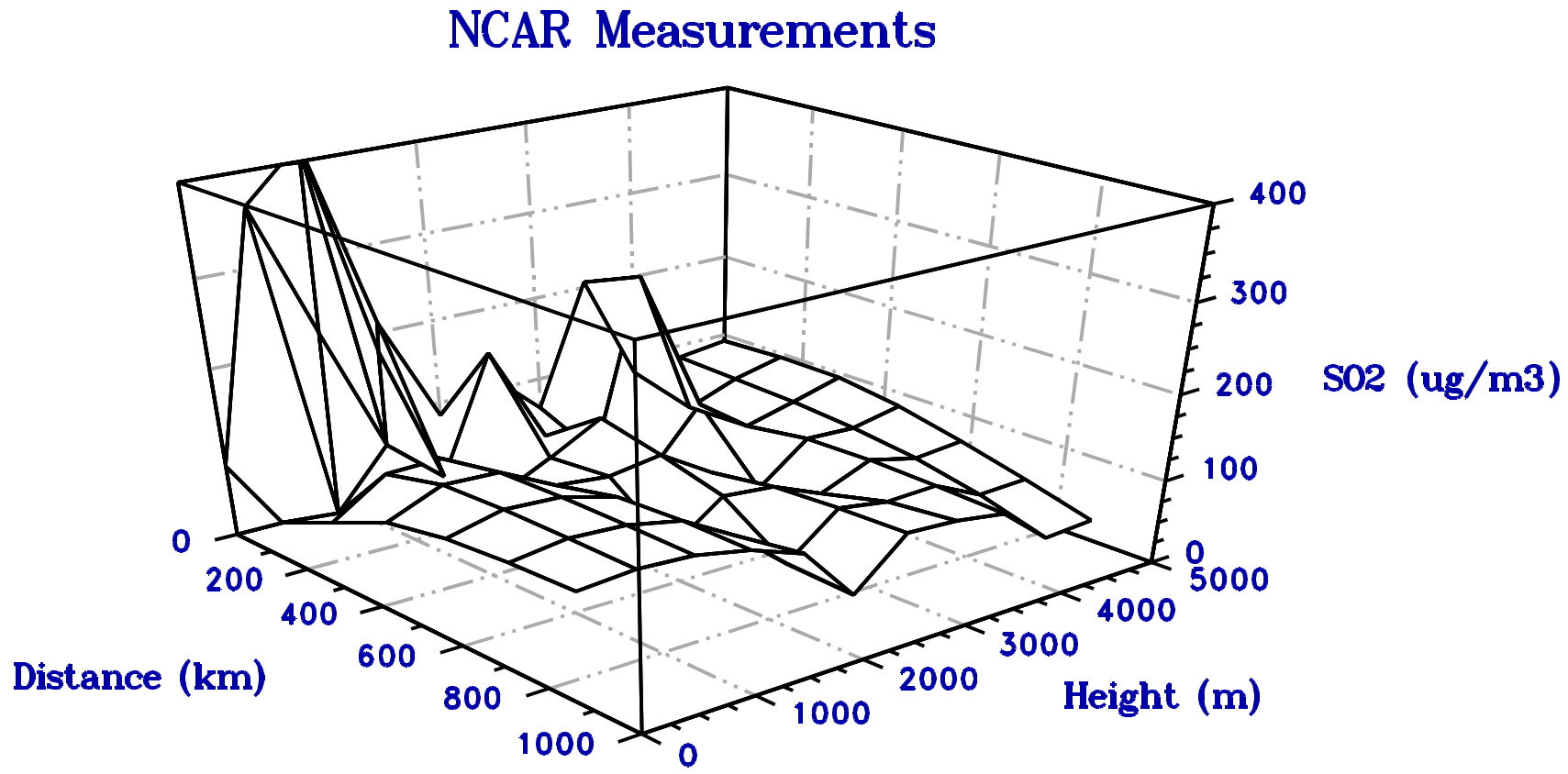

Figure 10. Composite SO_2 plume illustration from measurements taken by the NCAR aircraft averaged by downwind distance and height.

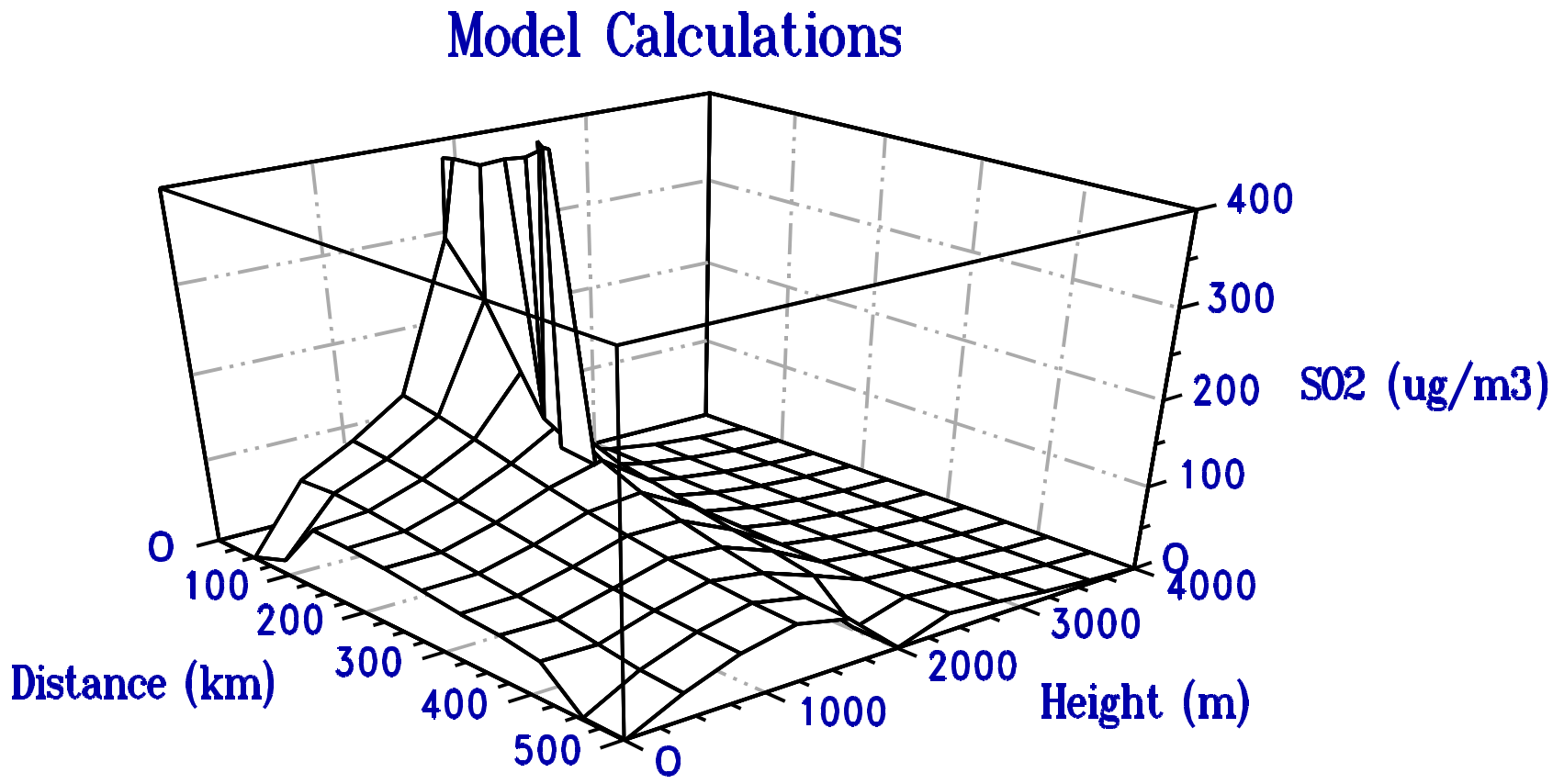

Figure 11. Model calculated SO_2 plume averaged over the days corresponding to the NCAR aircraft measurements.

Figure 12. Map showing location of ground-level SO_2 sampling locations.

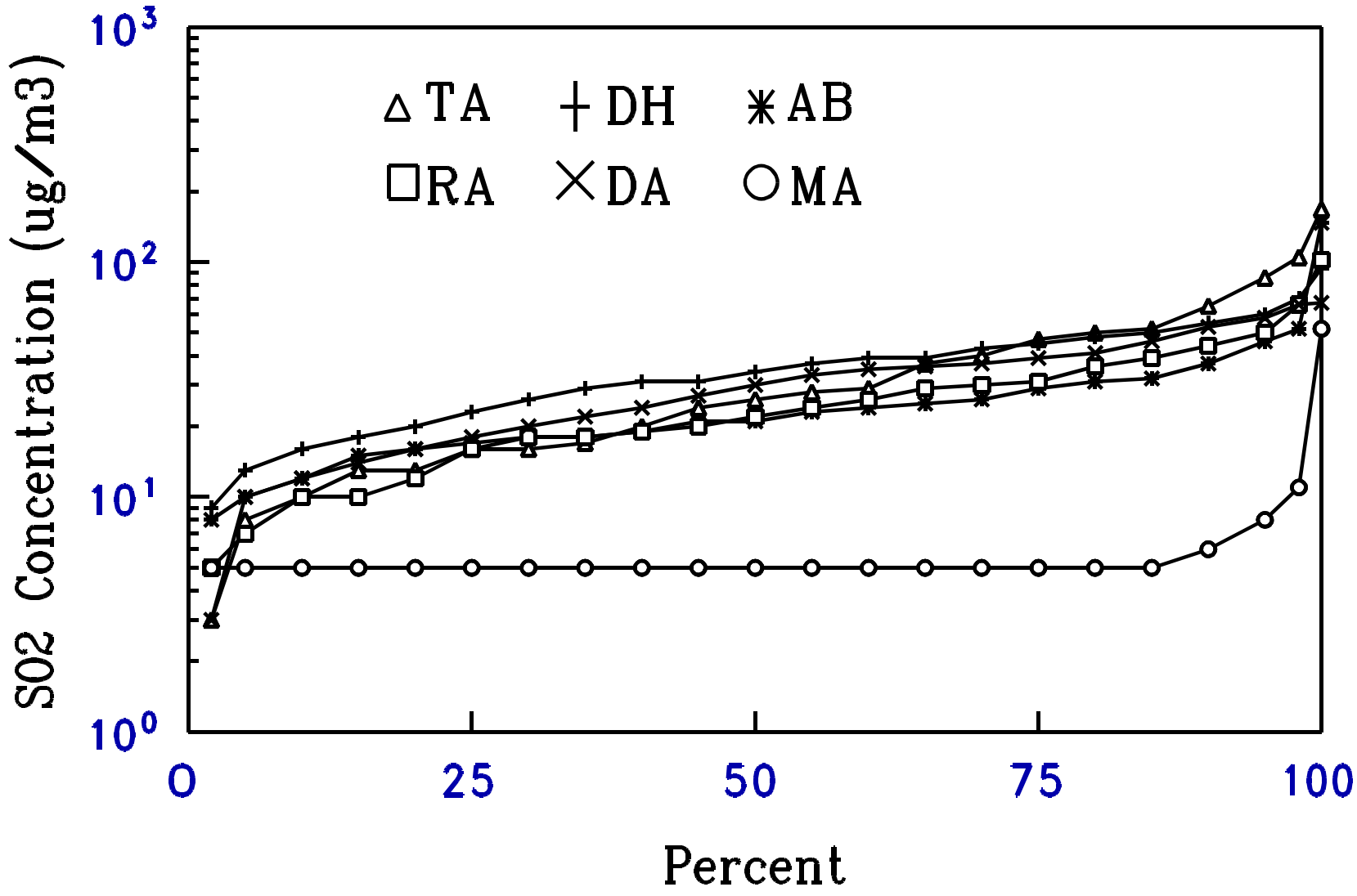

Figure 13. Cumulative SO_2 air concentration probability distributions at Tanajib (TA), Dhahran (DH), Abqaiq (AB), Rahimah (RA), Damman (DA), and Mansouriya (MA).

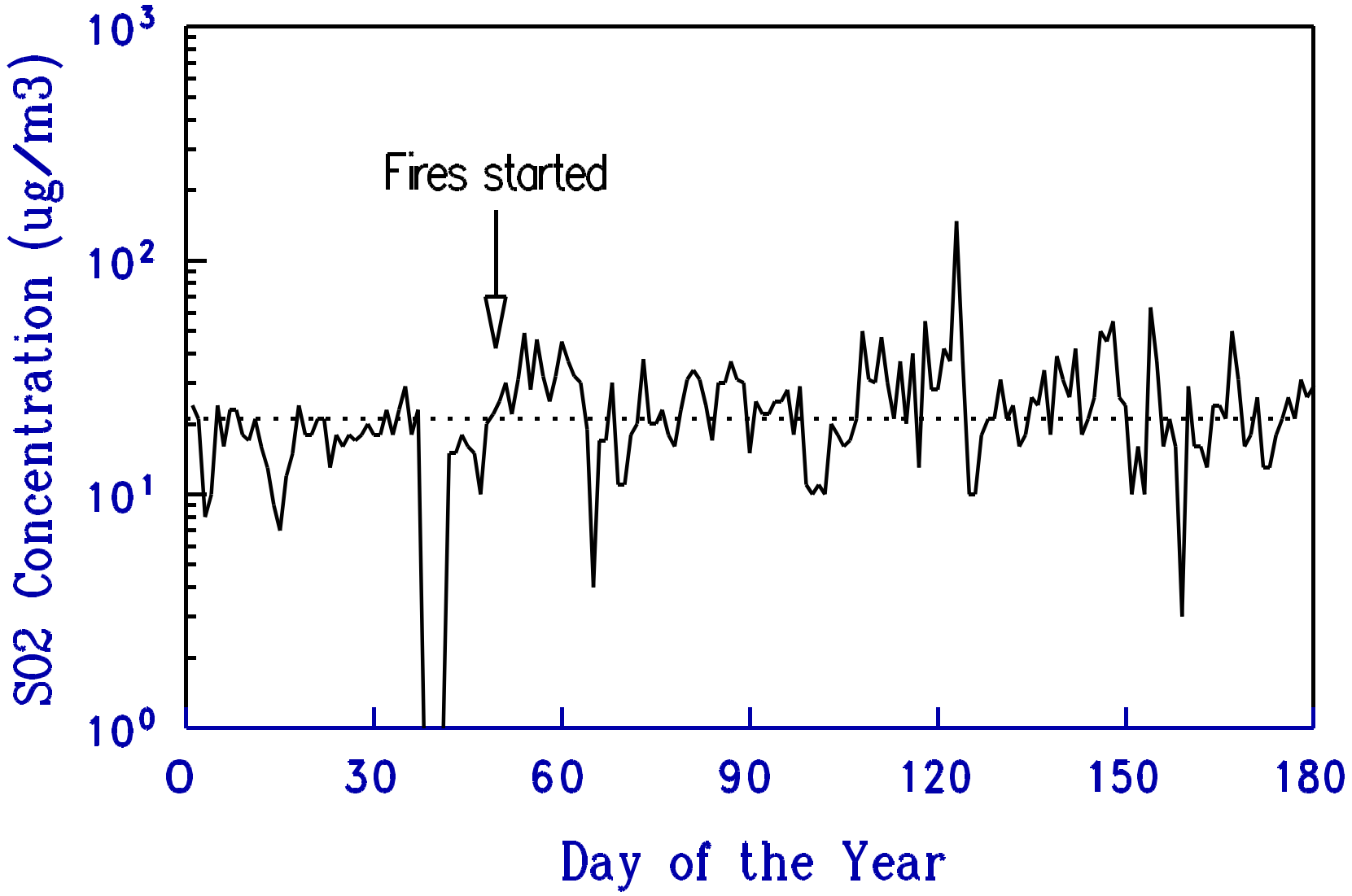

Figure 14. Time series of daily ground-level SO_2 measurements at Abqaiq. Dotted line represents the post-fires estimated background concentration, which is defined as the median concentration for the data shown in this illustration.

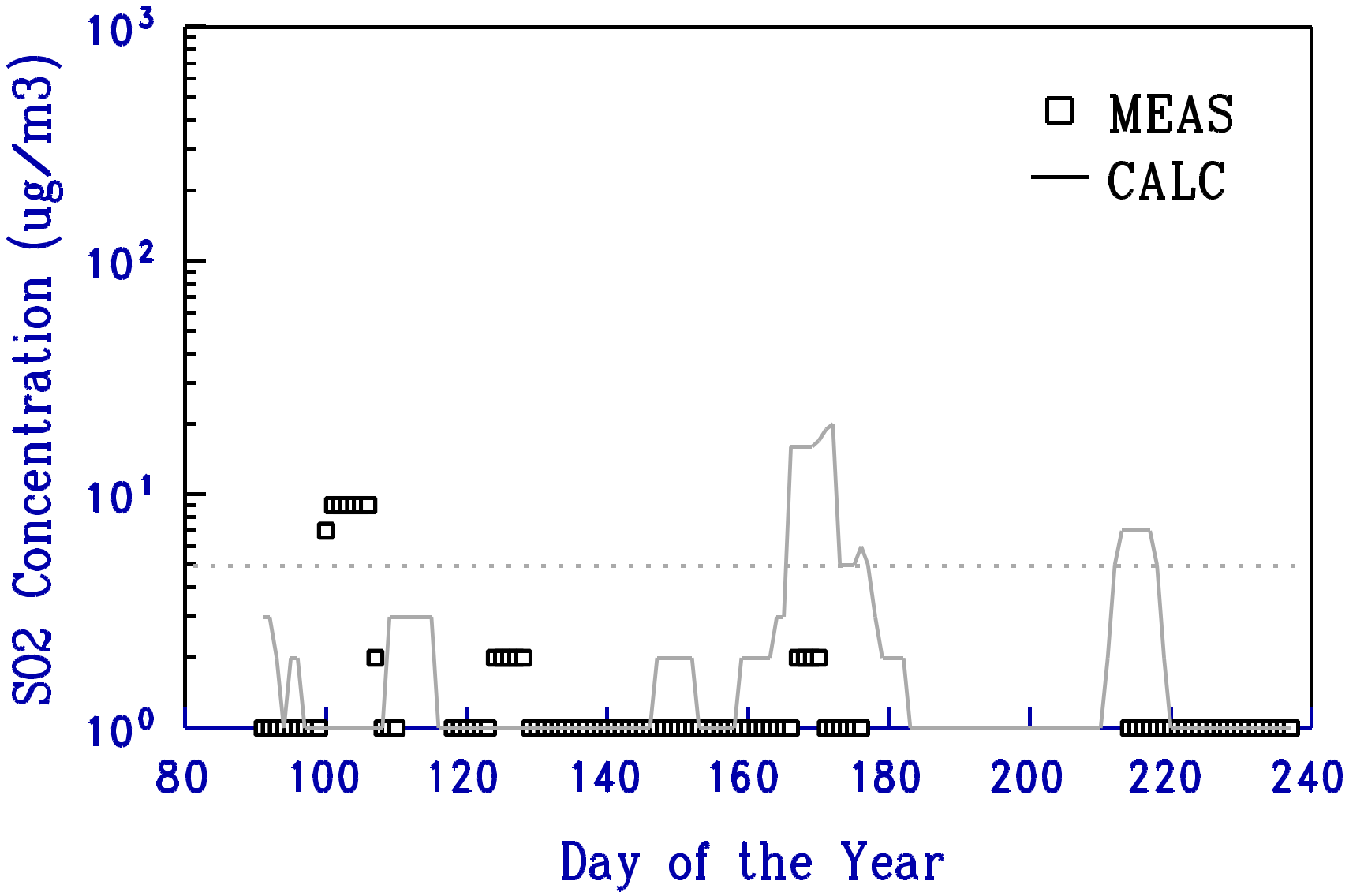

Figure 15. Time series of weekly above-background measured and calculated SO_2 concentrations at the near-source ground-level sampler (Mansouriya). A background of 5 (dotted line) has been subtracted.

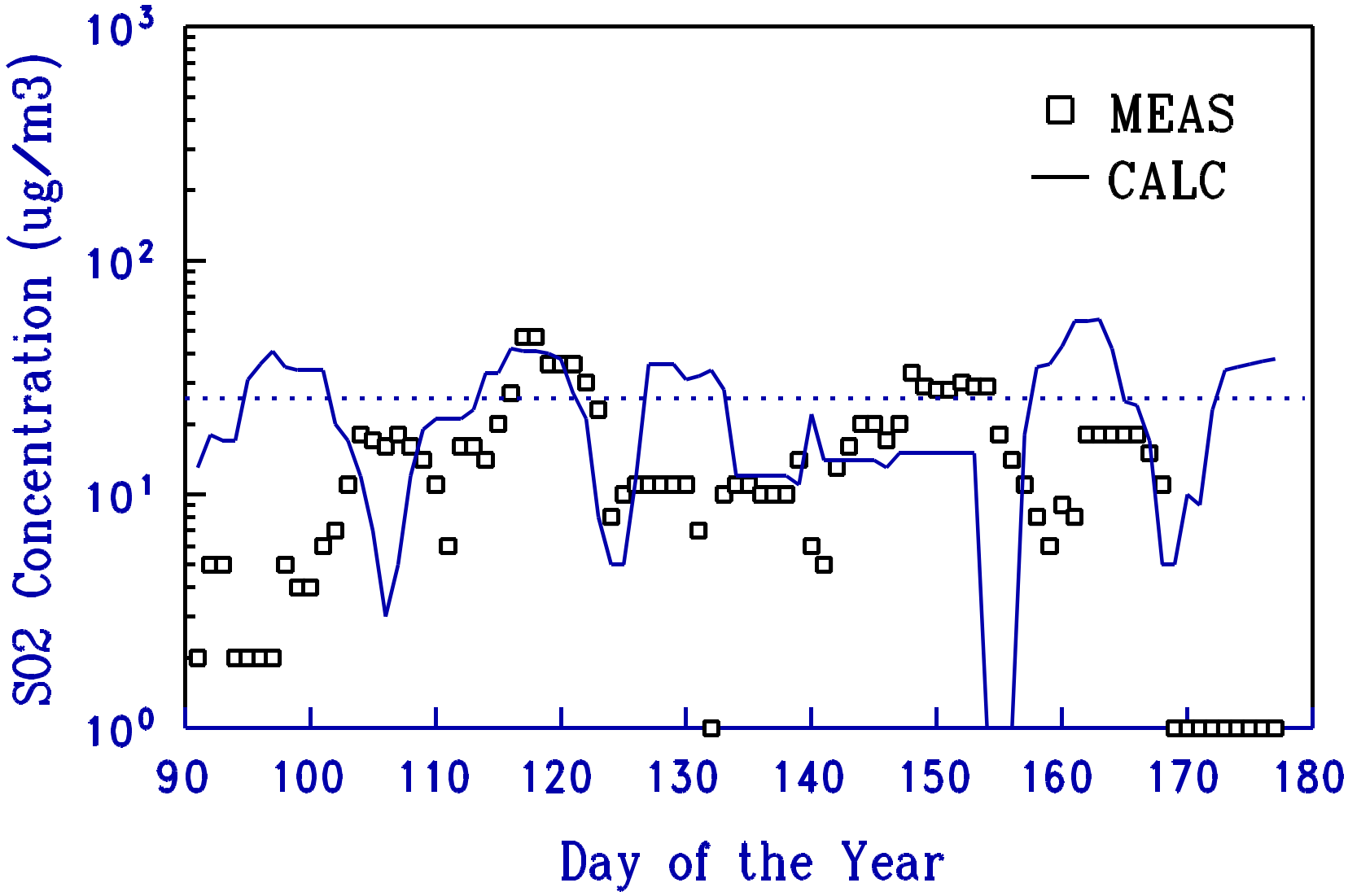

Figure 16. Time series of weekly above-backgound measured and calculated SO_2 concentrations at the mid-distance ground-level sampler (Tanajib). A background of 26 (dotted line) has been subtracted.

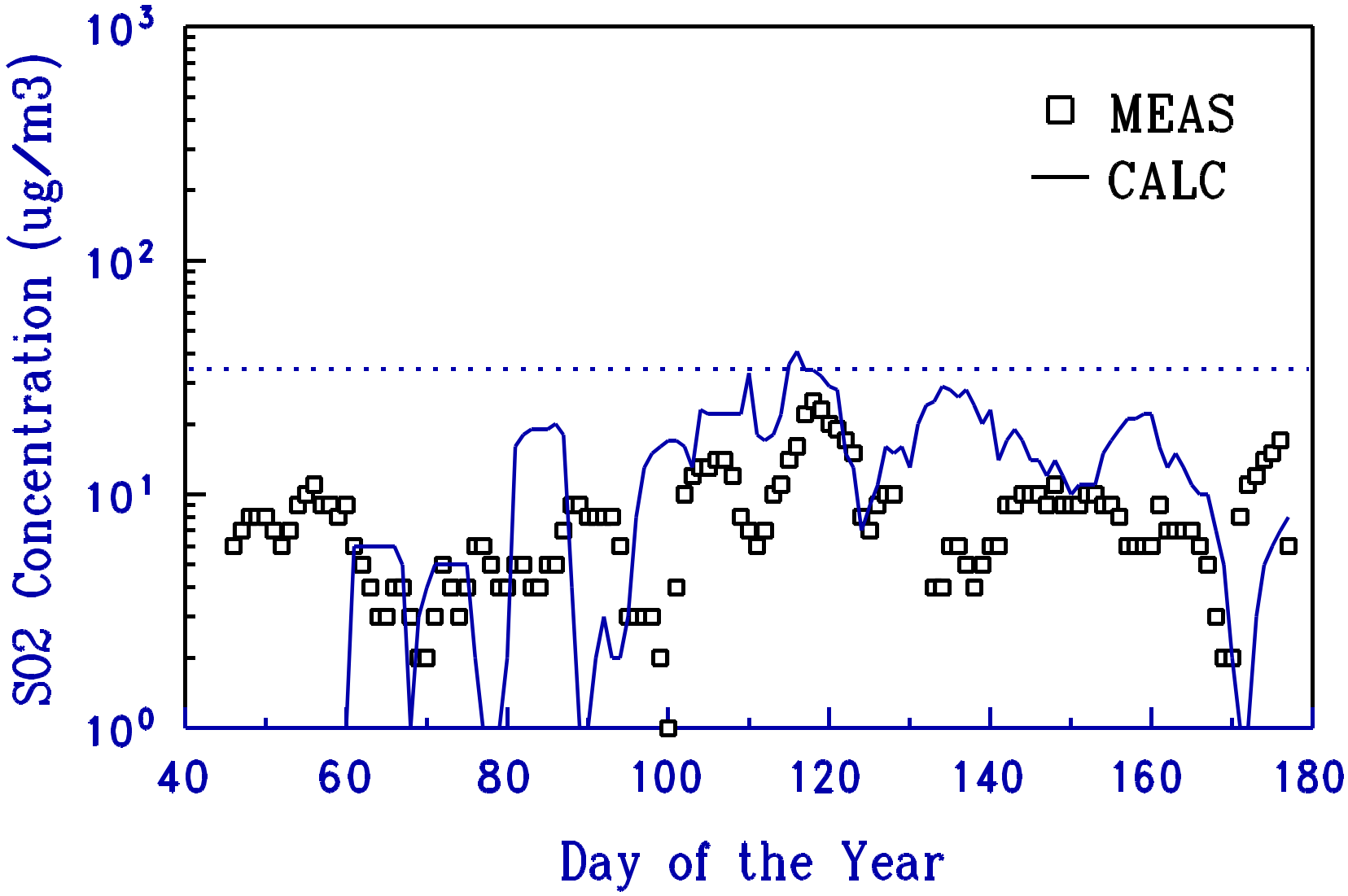

Figure 17. Time series of weekly above-background measured and calculated SO_2 concentrations at the far-downwind ground-level sampling location (Dhahran). A background of 34 (dotted line) has been subtracted.